STATE ESTIMATION OF POWER SYSTEM CONSIDERING THERMAL STATES OF TRANSMISSION LINE AND POWER TRANSFORMER

DUMRONGSAK WONGTA

A Dissertation Submitted to University of Phayao

in Partial Fulfillment of the Requirements

for the Doctor of Philosophy Degree in Electrical Engineering

October 2024

การประมาณสถานะของระบบไฟฟ้ากำลังที่มีการพิจารณาสถานะความร้อนของสายส่งและหม้อแปลงกำลัง

ดำรงศักดิ์ วงศ์ตา

วิทยานิพนธ์เสนอมหาวิทยาลัยพะเยา เพื่อเป็นส่วนหนึ่งของการศึกษา
หลักสูตรปริญญาปรัชญาดุษฎีบัณฑิต
สาขาวิชาวิศวกรรมไฟฟ้า
ตุลาคม 2567

STATE ESTIMATION OF POWER SYSTEM CONSIDERING THERMAL STATES OF TRANSMISSION LINE AND POWER TRANSFORMER

DUMRONGSAK WONGTA

A Dissertation Submitted to University of Phayao

in Partial Fulfillment of the Requirements

for the Doctor of Philosophy Degree in Electrical Engineering

October 2024

Dissertation

Title

State Estimation of Power System Considering Thermal States of Transmission Line and Power Transformer

Submitted by DUMRONGSAK WONGTA

Approved in partial fulfillment of the requriements for the

Doctor of Philosophy Degree in Electrical Engineering

University of Phayao

Approved by

..... Chairman

(Associate Professor Sanchai Dechanupaprittha , Ph.D.)

..... Advisor

(Associate Professor Chawasak Rakpenthai , Ph.D.)

..... Co Advisor

(Associate Professor Jonglak Pahasa , Ph.D.)

..... Co Advisor

(Associate Professor Sermsak Uatrongjit , Ph.D.)

..... External Examiner

(Associate Professor Sitthidet Vachirasricirikul , Ph.D.)

..... Dean of School of Engineering

(Associate Professor Nattapong Damrongwiriyanupap , Ph.D.)

Title: STATE ESTIMATION OF POWER SYSTEM CONSIDERING THERMAL STATES OF TRANSMISSION LINE AND POWER TRANSFORMER

Author: Dumrongsak Wongta, Dissertation: Ph.D. (Electrical Engineering), University of Phayao, 2024

Advisor: Associate Professor Chawasak Rakpenthai , Ph.D. Co-advisor Associate ProfessorJonglak Pahasa , Ph.D. Associate ProfessorSermsak Uatrongjit , Ph.D.

Keywords: States Estimation Conductor Temperature Transformer Parameters Top – Oil Temperature Hot – Spot Winding Temperature Three – Phase Networks

ABSTRACT

The problem of the voltage stability assessment considering the thermal limit of the transmission line has been addressed in this dissertation. Two indicators, namely line voltage stability and line ampacity indices, to determine the voltage stability states and line security of power systems under various operating conditions have been proposed. Both indices rely on the measured values that are already obtained from conventional measurements used in power systems. The identification of weak buses and critical lines based on the proposed indices is possible using only voltage magnitude and real power measurements. Numerical experimental results on two power networks have been tested under increasing system loading and line outage conditions indicate that by considering both line voltage stability and line ampacity indices, power systems could mitigate the risks of voltage collapse and excessive current in transmission lines. The influence of the thermal states of the transmission line and the power transformer on state estimation of electric power systems has also been studied. The three – phase state estimation algorithm based on the weighted least square method has also been proposed. The node admittance matrix model of the three – phase transformer and the weather – dependent thermal model of the overhead transmission line are integrated into the state estimation problem. It is then formulated as a nonlinear optimization with equality and inequality constraints. The estimated state variables consist of the bus voltage phasors, the transformer parameters, the transmission line conductor temperatures, and the weather states. Then, the top – oil and the hot – spot winding temperatures of the transformers can be evaluated using the estimates states. The IEEE 30 – bus and 118 – bus systems have been modified as three – phase test systems and the numerical results indicate that the proposed state estimation can be used to estimate the thermal states of the transmission line and the power transformers and the accuracy of the estimated states is also improved.

ACKNOWLEDGEMENT

This dissertation has been successfully completed with great appreciation and gratitude to Associate Professor Dr.Chawasak Rakpenthai, the dissertation advisor, Associate Professor Dr.Sanchai Dechanupaprittha, Associate Professor Dr.Jonglak Pahasa, Associate Professor Dr.Sermsak Uatrongjit, and Associate Professor Dr.Sitthidet Vachirasricirikul.

The dissertation committee members, for their valuable advice, guidance, and continuous support throughout the research process. The researcher expresses sincere gratitude for their invaluable assistance and close monitoring of the progress. I respectfully express my gratitude to all experts for their valuable feedback and suggestions to improve the research tools, as well as to the knowledgeable individuals who generously contributed their time to provide insightful interviews on the research direction. Additionally, I would like to thank all faculty members of the engineering faculty and every staff member for their support.

Finally, the researcher would like to express sincere gratitude to his family, who has been a significant source of motivation and support throughout the completion of this dissertation. Special thanks also go to colleagues, seniors, and juniors in the engineering field, as well as to everyone else who has provided invaluable assistance and encouragement to the researcher throughout this journey.

Dumrongsak Wongta

LIST OF CONTENTS

Page

LIST OF TABLES

Page

LIST OF FIGURES

Page

Chapter I

Introduction

Background and Motivation

The power system state estimation is a critical process in the analysis and management of power systems. This entails utilizing partial measurement data to estimate the state variables of a power system that cannot be measured directly [1]. Transmission lines are essential components of power grids that are responsible for transmitting electrical power over long distances from generating stations to distribution substations and end users. The temperature of conductors on transmission lines is directly proportional to the current flowing through them and is influenced by various factors for the operation and efficiency of power systems. Temperature has a significant impact on the performance and lifespan of power transformers that are designed to operate within specific temperature limits to ensure optimal performance and longevity. High temperatures can lead to accelerated aging and degradation of insulation materials, which are crucial for maintaining electrical insulation and preventing electrical breakdown within transformers.

Monitoring the temperature of conductors in transmission lines and that of power transformers [2 – 5], is crucial for ensuring reliable and efficient operation of the power system. High temperatures in conductors can lead to increased power loss, thermal expansion, conductor sagging, and reduced power transmission capability. Analyzing in the power system to determine the safety margin of transmission lines helps to evaluate and analyze the system's ability to maintain voltage levels within safe and stable limits under various operating conditions. This involves considering potential scenarios that could cause the voltage levels to exceed specified limits, which could compromise the overall safety and stability of the power system. Determining the safety margin of transmission lines involves analyzing and simulating the system using computational modeling software to assess power flow equations under various system conditions, using numerical indices and indicators to estimate electrical parameters, evaluate voltage levels, and ensure that the current flow in transmission lines remains at safe levels.

Power system state estimation algorithms assume that transmission lines and power transformers operate under normal conditions, and that their thermal limits do not exceed [6]. power systems experience higher stress levels and operate closer to their thermal limits [7]. This can lead to situations in which transmission lines and power transformers operate in states in which their thermal limits are violated, potentially compromising the reliability and security of the power system.

Therefore, there is a need to develop state estimation algorithms that consider the thermal states of the transmission lines and power transformers. By incorporating thermal constraints into the state estimation process, it is possible to accurately assess in the impact of thermal limitations on the operating state of the power system. This enhanced state estimation capability can help operators make informed decisions to ensure reliable and secure operation of the power system, even under stressed conditions. In addition, considering the thermal states of transmission lines and power transformers in state estimation can facilitate better asset management and preventive maintenance, leading to improved overall system reliability and efficiency.

Literature Review

Qingwen, *et al.* [8] presented transmission line parameters, which vary with temperature and affect the accuracy of state estimation of the power system, using in the principle of electro thermal coordination state estimation (ETC – SE). This study introduces two methodologies that consider the temperature variability of the transmission lines. Method 1 combines the heat balance equation and least – squares method with the Jacobian model. The heat balance equation and the temperature of the transmission line are integrated into the state vector. Additional enhancements to the Jacobian matrix enable the calculation of the conductor temperature and voltage phasors, providing coefficients for the transmission line temperature. This paper presents a two – step improvement technique in which the system state estimation and temperature are decoupled and solved through iterative procedures. Validation using IEEE 14 – bus, 39 – bus, and 118 – bus systems demonstrated the effectiveness of the proposed

methods in reducing calculation errors and ensuring robust processing performance under changing environmental conditions and in cases of ill – conditioned branches.

Cho, et al. [9] improved the accuracy of a methodology implementing state estimation in large – scale power systems with a partial reliance on variable renewable energy sources. The proposed state estimation method focuses on determining the state of the power system, including those that integrate wind and solar power systems. The methodology is a fast – decoupled weighted least – squares approach based on the common database of the application. In this methodology, renewable energy modeling considers various factors such as the same data, type of renewable energy source, and voltage level of the bus connected renewable energy. Additionally, the proposed algorithm incorporates precise bad data processing techniques that utilize inner and outer functions. The inner function employs the normalized residue method for bad data detection, identification, and adjustment, whereas the outer function assesses whether they have been identified. To reduce measurement errors associated with transformers, a connectivity model has been introduced for transformers employing switching devices. Simple method for transformer error processing. The effectiveness of the proposed methodology was tested based on the IEEE 18 – bus system, which integrates a large – scale power system with renewable energy sources.

Fulin, et al. [10] presented the impact of measurement errors on the real – time thermal rating estimation for overhead lines. Introducing a Monte Carlo based approach to model the propagation of measurement uncertainties in estimates has contributed to an effective investigation of two weather condition approaches to estimating from inference or measurement of conductor temperature, flowing current in the conductor, and weather variables, as demonstrated by the name Drake of the conductor specification. The accuracy of the model increases with an increase in conductor temperature above the ambient temperature. In addition, the effective wind speed and solar radiation were adjusted. The proposed methods were tested based on two spans comprising different types of conductors, the sensor specification based limits, with an enhanced based approach that models transient changes in the conductor temperature in each scenario.

Marija, *et al.* [11] presented a state estimation in modern control centers, serving as a crucial tool for enhancing the reliability and effectiveness of power system operations. Improved accuracy in state estimation leads to a more reliable representation of the power system, and investigates the impact of temperature induced changes in transmission line resistance on the performance of state estimation. By integrating the line heat balance equation and weather data, this study accounts for this effect in state estimation. The findings reveal that temperature induced changes in the transmission line resistance have a notable impact on the accuracy of the state estimation. Adjusting the resistance of the power transmission grid model to match specific weather and loading conditions can enhance the accuracy of state estimation results. The proposed approach offers practical implementation potential because it enables a more precise allocation of transmission losses and facilitates the accurate determination of power flows and network voltage profiles.

Olav, *et al.* [12] presented that the significant challenge faced by utilities in assessing the remaining life of distribution transformer insulation is the lack of recorded load or temperature data, which are essential inputs for remaining insulation life algorithms. This absence of critical data impedes the application of such algorithms, thereby limiting their ability to accurately predict insulation life. In power flow studies, state estimation methods play a crucial role in determining the power flow across a network. This article presents a study in which state estimation techniques were employed to estimate the load of a specific distribution transformer within a network. By extrapolating from this load estimation, it was possible to estimate the insulation temperature and remaining life of the transformer. The preliminary results of this study are highly promising, indicating the potential utility of employing state estimation techniques for estimating the transformer load and, subsequently, the remaining insulation life. Further measures are planned to validate and refine this methodology with the aim of enhancing its practical applicability in real world utility scenarios.

Kourosh, *et al.* [13] presented the critical impact of localized temperature elevation, specifically focusing on the hottest spot temperature, which can lead to the rapid thermal degradation of insulation and subsequent thermal breakdown in

transformers. Accurately estimating the hottest spot temperature of transformer windings is imperative for determining both short – term and long – term loading capabilities. The research presented in this paper contributes to enhancing the accuracy of the hottest spot temperature estimation, thereby enabling more precise assessments of transformer performance under varying load conditions. Recognizing that an excessive temperature rise resulting from load currents is a primary driver of insulation degradation in power transformers, accurate estimation of parameters such as the top – oil temperature and hot – spot temperature becomes paramount. Among other standards organizations, IEEE and IEC have proposed methodologies for estimating these temperatures, underscoring the industry wide recognition of the importance of this issue. By refining existing estimation techniques and exploring novel approaches, this study aims to advance the understanding of transformer behavior under different loading scenarios and facilitate more informed decision making regarding transformer operation and maintenance.

Almohaimeed, *et al.* [14] presented the impact of global climate change, particularly on distribution transformers, the implications of changing ambient temperatures and operating conditions on the performance and longevity of distribution transformers. A case study was conducted using real world data from Chicago, Illinois, to investigate the effects of the ambient temperature variations and operational temperatures on the functionality and lifespan of distribution transformers. This study aims to optimize transformer performance under changing environmental conditions. By analyzing in the impact of increasing ambient temperatures on the operational lifespan of distribution transformers in this specific urban environment, valuable insights are gained into the challenges posed by climate change to the transformer infrastructure. Using advanced modeling techniques, predictive analytics, and adaptation strategies, this study aims to contribute to the development of robust solutions for enhancing the resilience and sustainability of distribution transformer networks in the context of evolving climate conditions.

Chawasak, *et al.* [15] presented a state estimation methodology tailored for three phase power systems, where the states included bus voltage phasors, considering the conductor temperature of the transmission line. The transmission line admittance

parameters, contingent upon the line conductor and ambient temperature, are estimated using precomputed data and polynomial interpolations. Incorporate of the temperature estimation into the state estimation process, weather environmental variables, and heat – balance equations into the measurement functions. In addition, a technique for segmenting transmission lines is employed to effectively handle temperature variations in the distance between transmission lines. The state estimation problem is a constrained nonlinear optimization task based on the weighted least – squares criterion. The solution was derived using a predictor–corrector interior point algorithm. Simulation results conducted on several three – phase power systems demonstrate that the proposed methodology delivers estimations with enhanced accuracy compared with existing techniques.

Ossama El – Sayed, *et al.* [16] presented a method for predicting the temperature increase and loss of life in transformers under the influence of harmonic load currents. The model considers parameters that affect a transformer's life expectancy, including the hot – spot winding and top – oil temperature. It utilizes a model for the top – oil and hot – spot temperature rise over the ambient temperature, as well as a thermal model for both linear and non – linear loads. The hot – spot winding, top oil, and loss of life of a power transformer under a harmonic load are calculated. The models were applied to 25 MVA and 66/11 kV transformer units at varying loads, and the results were compared with the measured temperature results. The results obtained by the IEEE model are also very good for the hot – spot winding temperature calculation, but less accurate for the top – oil temperature. The top – oil and hot – spot winding temperatures with and without harmonic loads are calculated under a constant load, which shows that the top – oil temperature in a transformer with harmonic current is greater than without by 10, and the hot – spot winding temperature by 13. The increase in the transformer temperature would lose all of its life in half of its chosen normal life.

Purposes of the Study

1. To develop an algorithm for state estimation of power systems that considers thermal states of the transmission line and the power transformer.

2. To improve the performance of the state estimation.

Research Scope

The incorporation of the thermal states of the transmission line and the power transformer into the algorithm can lead to improved accuracy and effectiveness in power system state estimation.

Research Methodologies

1. Study the power flow problem that considers the thermal states of the transmission line and the power transformer.

2. Study the state estimation problem of three – phase power.

3. Study the thermal modelling of power components of power system.

4. Propose the state estimation algorithm which can be used to estimate the thermal states of the transmission line and the power transformer.

5. Develop the state estimation using the MATLAB program.

6. Test the performance of the proposed algorithm on three – phase test networks.

Research Contributions

The main contributions of this dissertation listed as follows.

– The line voltage stability and the line ampacity indices have been presented based on power flow formulation in order to evaluate the bus voltage stability and the transmission line thermal levels in power systems under various operations. Both indices can be computed using only bus voltage magnitudes and real power flow measurements obtained from the conventional measurements.

– The three – phase state estimation algorithm for power systems in which state variables are the bus voltage phasors, the transformer parameters, and the conductor temperatures of lines, has been proposed. The state estimation has been formulated as a nonlinear constrained optimization problem based on the weighted least square method. The estimated state variables can also be used to estimate the top – oil and the hot – spot winding temperatures of power transformer.

Dissertation Organization

The dissertation is organized as follows:

1. Chapter 1 introduces the importance of state estimation for power systems considering the thermal state of the transmission line and the power transformer. Mention – related background and motivation, literature review, and stating the purpose of the study, research scope, research methodologies, and research contributions.

2. Chapter 2 establishes research on the assessment of power system voltage stability considering transmission line security. Develop equations based on the power flow. There are two indices for network testing that determine the voltage collapse points, weak buses and security lines. and were compared with the other voltage stability indices.

3. Chapter 3 explains the transmission line thermal modeling according to the IEEE standard 738 – 2012 using the concept of a heat – balance equation. The temperature of overhead transmission line varies based on the surrounding environmental conditions. The effective value of the current flowing in the transmission line affects the temperature change. The thermal modeling of power transformer according to IEEE C57.91 – 2011 is also described. The thermal state estimation equations developed based on the thermal models of the transmission line and the power transformer are presented.

4. Chapter 4 presents the state estimation method for estimating the thermal states of the transmission line and the power transformer of power system. Testing on two three – phase power networks are demonstrated.

5. Chapter 5 concludes the work presented in this dissertation and gives the recommendations of further research directions.

Chapter II

Transmission Line Thermal Limit and Voltage Stability

Introduction

As electrical energy consumption and the integration of renewable sources continue to rise, operation of power systems has become a complex task involving both economic and security constraints. The disturbances in power systems, such as a sudden increase in load, transmission line outage, generator failure, and the intermittent nature of renewable energy sources, have the potential to reduce the voltage stability margin. Consequently, the maximum power that can be supplied to the load bus without breaching voltage limits also diminishes. Without appropriate estimation and mitigation strategies for the voltage stability problem, voltage collapse may occur in power systems which can result in severe damage to the network [17] and potentially lead to an electrical blackout. Thus, the assessment of the voltage stability in power systems under various operating conditions has become of the utmost importance. Several voltage stability indicators, which play essential roles in identifying critical locations within power networks where voltage collapse may originate, have been developed. Voltage stability indices based on the maximum loading conditions of a two – bus system have been presented in [18 – 23].

The transmission line parameters and some system variables such as bus voltages and power flow through lines are used to formulate the indices. These indicators require minimal computational effort, making them suitable for rapid identification of systems operating under changing loads and contingency conditions. However, due to some assumptions in these indices, different and unpredictable values can be obtained when they are applied to large – scale power networks [24 – 26]. Other indices based on the Jacobian matrix of load flow analysis have been presented. An index based on the minimum singular value decomposition of the Jacobian matrix has been presented in [27]. The maximum singular value of the inverse Jacobian matrix and its derivative has been presented in [28]. This index is approximately linear and can determine the voltage stability margin. A model analysis – based index based on the minimum eigenvalue and

right eigenvector of the Jacobian matrix has been presented in [29]. The voltage stability of system occurs when all eigenvalues are positive. The maximum element of system tangent vector, which are the sensitivity of state variables including the bus voltage magnitudes and angles with respect to the load variation, has been presented in [30]. The inverse of the maximum element of the tangent vector is close to zero at the voltage collapse point. A test function based on the reduction of the Jacobian matrix with respect to the critical bus of system has been presented in [31]. This index can be used to predict the voltage collapse point by fitting the test function using a quadratic model. Test results in [31] also show that the minimum singular value and the eigenvalue of Jacobian matrices proposed in [27] and [29] are not good indicators due to their nonlinear behaviors when the bus voltage magnitude approaches its collapse point. In addition, these techniques require rather time consuming computation steps and may not be suitable for implementation in realistic power systems because accurate parameters are required for system models. In [32 – 38], indices based on Thevenin equivalent impedance of the rest of the power system using the data obtained from the measurement system, have been presented for real – time voltage stability assessment. The external Thevenin equivalent impedance has the same magnitude as the load impedance at the bus when the maximum loading condition occurred.

The point of voltage collapse is also the system operating point, at which the maximum available power can be delivered to the load. A systematic qualitative and quantitative comparison of some voltage stability indices based on the Thevenin equivalent obtained from estimated states using both conventional and measurements has been performed and reported in [39]. Therefore, this chapter develops equations using concepts of power flow for voltage stability assessment, considering the thermal limit. Simulation in IEEE networks can determine the voltage collapse point, weak buses and security lines.

Power Flow Equations

The power flow equations used to develop the proposed indicators are described. Figure 1, shows an equivalent π circuit of transmission line. The branch current phasor flowing from bus s to bus r can be obtained by

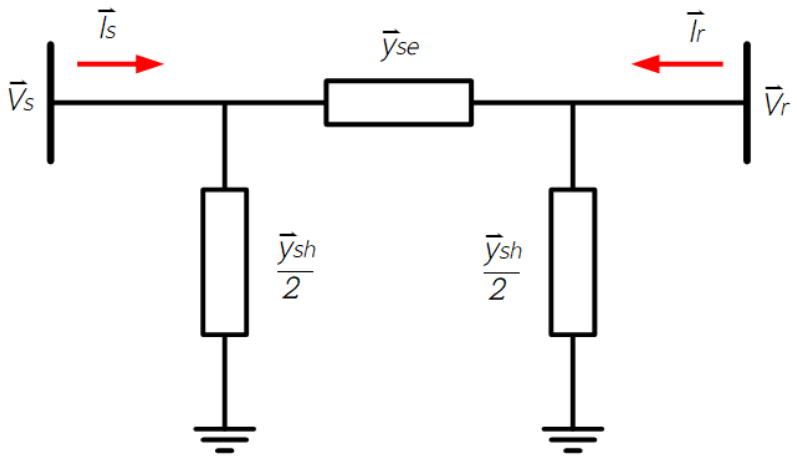

Figure 1 Equivalent circuit of transmission line.

$$\vec{I}_s = \left(\tfrac{1}{2}\vec{y}_{sh} + \vec{y}_{se}\right)\vec{V}_s - \vec{y}_{se}\vec{V}_r \tag{1}$$

where $\vec{I}_s = I_s\angle\theta_s$ is the current phasor at the sending end bus,

$\vec{V}_s = V_s\angle\delta_s$ is voltage phasor at the sending end bus,

$\vec{V}_r = V_r\angle\delta_r$ is voltage phasor at the receiving end bus,

$\vec{y}_{se} = g_{se} + jb_{se}$ is a series admittance of transmission line,

$\vec{y}_{sh} = g_{sh} + jb_{sh}$ is a shunt admittance of transmission line,

It is usually assumed that g_{sh} is zero.

A complex power flowing from the sending bus s to the receiving bus r, $\vec{S}_s$, can be calculated by

$$\vec{S}_s = P_s + jQ_s = \vec{V}_s\vec{I}_s^{*} \tag{2}$$

where P_s and Q_s are the real and reactive power flow from bus s to bus r, respectively. Note that the superscript * denotes a complex conjugation. Substituting (1) into (2), and separating into real and imaginary part, one obtains

$$P_s = g_{se}V_s^2 - V_sV_r\left(g_{se}\cos\delta + b_{se}\sin\delta\right) \tag{3}$$

$$Q_s = -\left(\tfrac{1}{2}b_{sh} + b_{se}\right)V_s^2 + V_sV_r\left(b_{se}\cos\delta - g_{se}\sin\delta\right) \tag{4}$$

where $\delta = \delta_s - \delta_r$ and g_{sh} is assumed to be zero. Similarly, the power flow from bus r to s can be computed by

$$P_r = g_{se}V_r^2 - V_sV_r\left(g_{se}\cos\delta - b_{se}\sin\delta\right) \tag{5}$$

$$Q_r = -\left(\tfrac{1}{2}b_{sh} + b_{se}\right)V_r^2 + V_sV_r\left(b_{se}\cos\delta + g_{se}\sin\delta\right) \tag{6}$$

where P_r and Q_r are the real and reactive power flow from bus r to bus s, respectively.

Proposed Indices

In this section, two indicators are proposed for assessing the voltage stability and line security of power networks. They are derived based on the real power flow through the transmission line and bus voltage magnitudes. The maximum loading condition that satisfies the limit of either indicator can be considered as a critical loading condition [40 – 42].

Line Voltage Stability Index

The line voltage stability index (LVSI) depends on influence of the power loading at the load bus. By considering the power flow from bus r to bus s, we can re – arrange (5) and formulate a quadratic equation in terms of a variable V_r as

$$g_{se}V_r^2 - KV_sV_r - P_r = 0 \tag{7}$$

where $K = g_{se}\cos\delta - B_{se}\sin\delta$ The roots of (7) are obtained as,

$$V_r = \left(KV_s \pm \sqrt{K^2V_s^2 + 4g_{se}P_r}\right) \Big/ 2g_{se} \tag{8}$$

Since the voltage magnitude V_r is a real number, the discriminant must satisfy the following condition,

$$K^2V_s^2 + 4g_{se}P_r \geq 0 \tag{9}$$

Moreover, (5) can be re – arranged as

$$V_s\left(g_{se}\cos\delta - b_{se}\sin\delta\right) = KV_s = \left(g_{se}V_r^2 - P_r\right) \Big/ V_r \tag{10}$$

Substituting (10) into (9), then we can define as the follows

$$\text{LVSI} = \frac{-4g_{se}V_r^2P_r}{(g_{se}V_r^2 - P_r)^2} \leq 1. \tag{11}$$

The value of LVSI closes one when the voltage magnitude at the receiving end bus approaches the voltage collapse point. The proposed LVSI requires only measurements of the bus voltage magnitude and the real power flow to determine voltage stability level under various operating conditions of power system.

Line Ampacity Index

Considering Figure 1, the real power loss of the transmission line can be obtained as follows

$$P_s + P_r = I_{se}^2 r_{se}, \tag{12}$$

where I_{se} is the magnitude of series current phasor of the line, and $r_{se} = g_{se} / (g_{se}^2 + b_{se}^2)$ represents line series resistance.

Substituting (3) and (5) into (12), one obtains

$$I_{se}^2 r_{se} = g_{se}\left(V_s^2 + V_r^2\right) - 2g_{se}V_sV_r\cos\delta \tag{13}$$

By using trigonometric identity, (5) can be re – written as

$$P_r = g_{se}V_r^2 - V_sV_r(g_{se}\cos\delta \pm b_{se}\sqrt{1-\cos^2\delta}) \tag{14}$$

Since $K = (g_{se}V_r^2 - P_r)/V_sV_r$, (14) can be re – arranged into the following equation

$$y_{se}^2\cos^2\delta - 2b_{se}K\cos\delta + \left(K^2 - b_{se}^2\right) = 0 \tag{15}$$

where $y_{se}^2 = g_{se}^2 + b_{se}^2$ is the squared magnitude of line's series admittance. Two values of $\cos\delta$ are obtained from (15). The one with larger magnitude is chosen since the phase difference of bus voltages phasors of the line is generally small. Hence, we obtain

$$\cos\delta = \left(g_{se}K + |b_{se}|\sqrt{y_{se}^2 - K^2}\right)/y_{se}^2 \tag{16}$$

Substituting (16) into (13), a series current magnitude flowing along transmission line can be expressed as

$$I_{se}^2 = y_{se}^2\left(V_s^2 + V_r^2\right) - 2V_sV_r\left(g_{se}K + |b_{se}|\sqrt{y_{se}^2 - K^2}\right) \tag{17}$$

From (17), we propose a line ampacity index (LAI) as

$$LAI = \frac{I_{se}}{I_{cr}} \leq 1 \tag{18}$$

where I_{cr} is the current rating of the transmission line. The value of LAI must be less than unity to maintain line security. The index value reaches one when the transmission line operates at its maximum loading condition. The proposed LAI requires only measurements of the bus voltage magnitudes and the real power flow to determine the security status of each line of power system. Critical line can also be identified based on the proposed index for power system operation under variations in loading and contingency.

Case Studies

In this section, the proposed assessment approach is demonstrated using two test systems. For each transmission line, LVSI and LAI proposed in the previous section are computed under various loading conditions. Both real and reactive powers at the base load are multiplied by a load scaling factor to simulate loading variation. The scaling factor is increased until the voltage collapse state occurs. The operating states of the test systems are simulated by using MATPOWER [43].

IEEE 2 – bus System

2 – bus system operated at 500 kV with a double – circuit transmission line. The line's length is set to 180 km and the phase conductor is assumed to be Hawk conductor. The real and reactive power loads at the receiving end are 340 MW and 285 MVAR, respectively. The voltage magnitude at the sending bus is fixed to be 1.0 p.u. while the voltage magnitude at the receiving bus depends on the loading conditions, as shown in Figure 2.

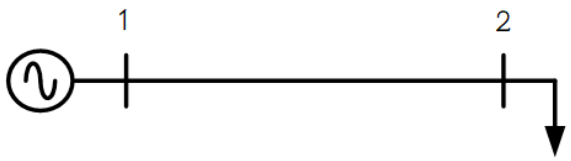

Figure 2 Single line diagram of 2 – bus system.

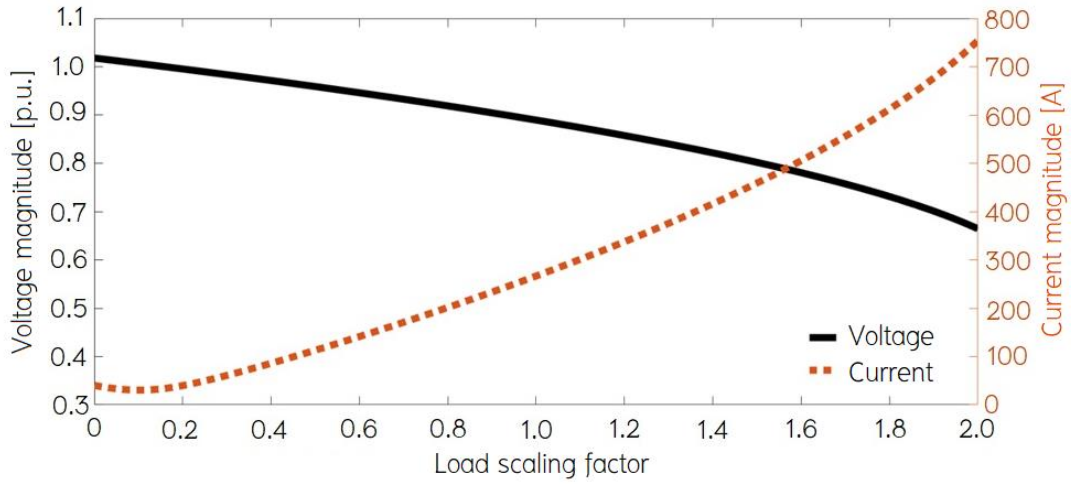

Figure 3 Voltage *and current magnitudes for 2 – bus system.*

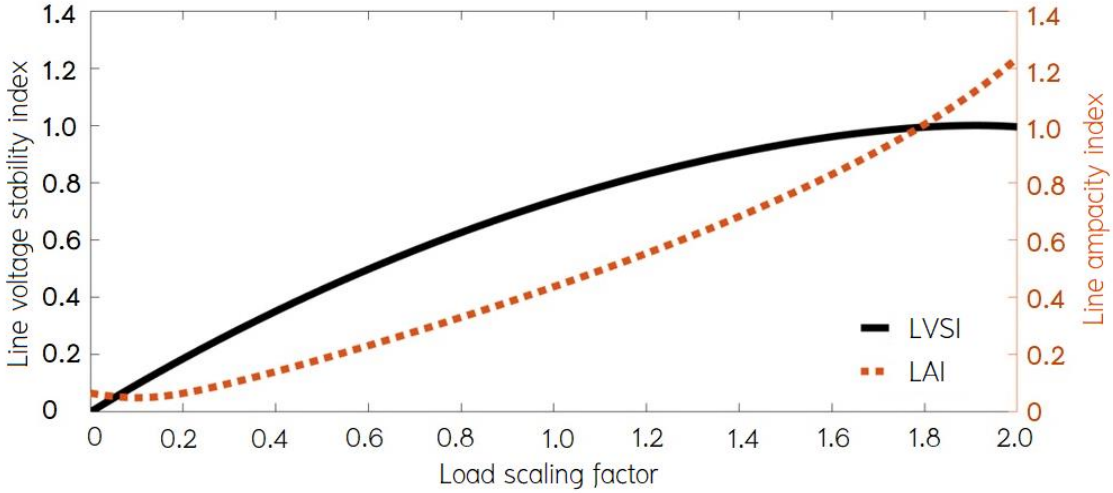

Figure 4 LVSI and LAI for 2 – bus system.

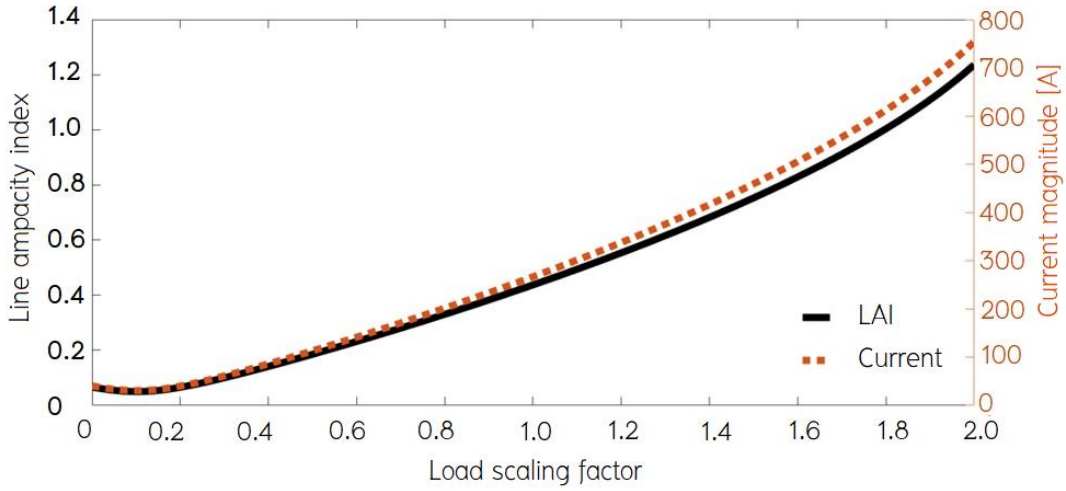

Figure 5 LAI and current magnitude for 2 – bus system.

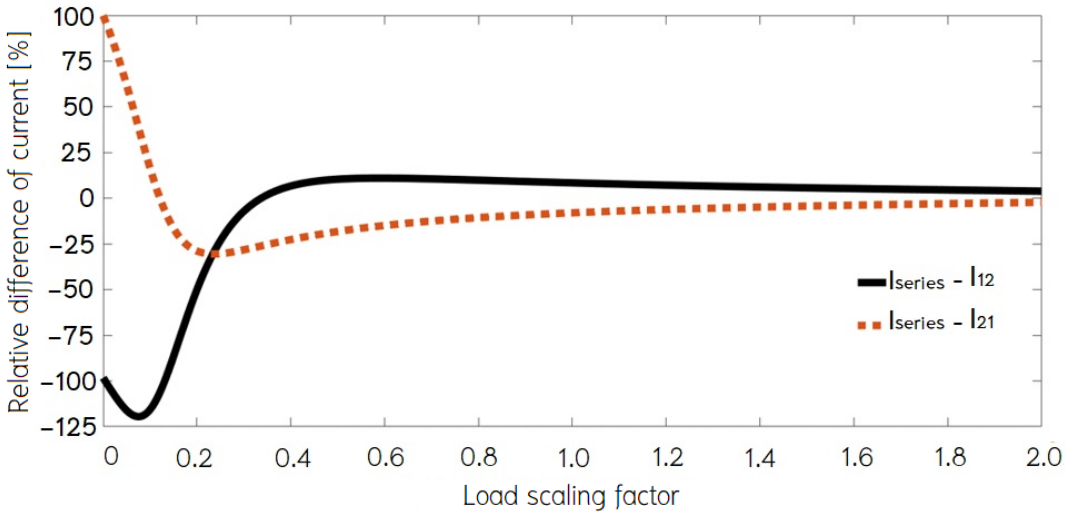

Figure 6 Difference of current magnitudes for 2 – bus system.

Figure 3, illustrates the voltage magnitude at the receiving bus and the series current magnitude on the phase conductor as functions of the load scaling factor. As the load increases, the current magnitude rises while the voltage magnitude declines. Although, the voltage collapse point occurs when the load scaling factor is 2, the current magnitude flowing though the conductor is approaching its current rating, that is 610 A, when the load scaling factor closes to 1.796. Therefore, the critical load scaling factor for

this situation is 1.796 to ensure transmission line security, as the current magnitude through the phase conductor remains below its current limit.

Figure 4, shows the bus voltage magnitude, the proposed LVSI and LAI of line with increasing load scaling factor. It can be observed that the value of the LVSI increases from 0 to 1 as load increases. The LVSI reaches its maximum value of 1.0 at the point of voltage collapse. Likewise, the value of the LAI also rises with an increase in loading. At the critical load scaling factor of 1.796, the LAI is 1.0 where the current magnitude of the phase conductor is equal to the current rating.

Figure 5, shows the relationship between the LAI and the series current magnitude as functions of the load scaling factor for the 2 – bus system. The value of LAI approaches unity when the series current magnitude is close to the current rating of the transmission line.

Figure 6, displays the percentage difference between the branch current magnitudes (I_{12} and I_{21}), which also includes effects of the series and shunt admittances, and the series current magnitude (I_{cr}), which considers only the series admittance of the transmission line. For large loads, where a significant proportion of the branch current is contributed by the series current phasors, the difference tends to zero.

IEEE 30 – bus System

In this subsection, the standard IEEE 30 – bus system has been modified as the test system. As shown in Figure 7, the system consists of 6 generators, 7 transformers, 41 lines, and 24 loads. Single – and double – circuit transmission lines are employed for 33 kV and 132 kV overhead lines, respectively. One conductor per phase is assumed except for line 21 – 22, where two conductors per phase are employed to enhance the line's carrying capacity. The phase conductors of the 33 kV and 132 kV overhead lines are assumed to be Panther and Hawk conductors, respectively. The line's length is chosen based on positive sequence reactance.

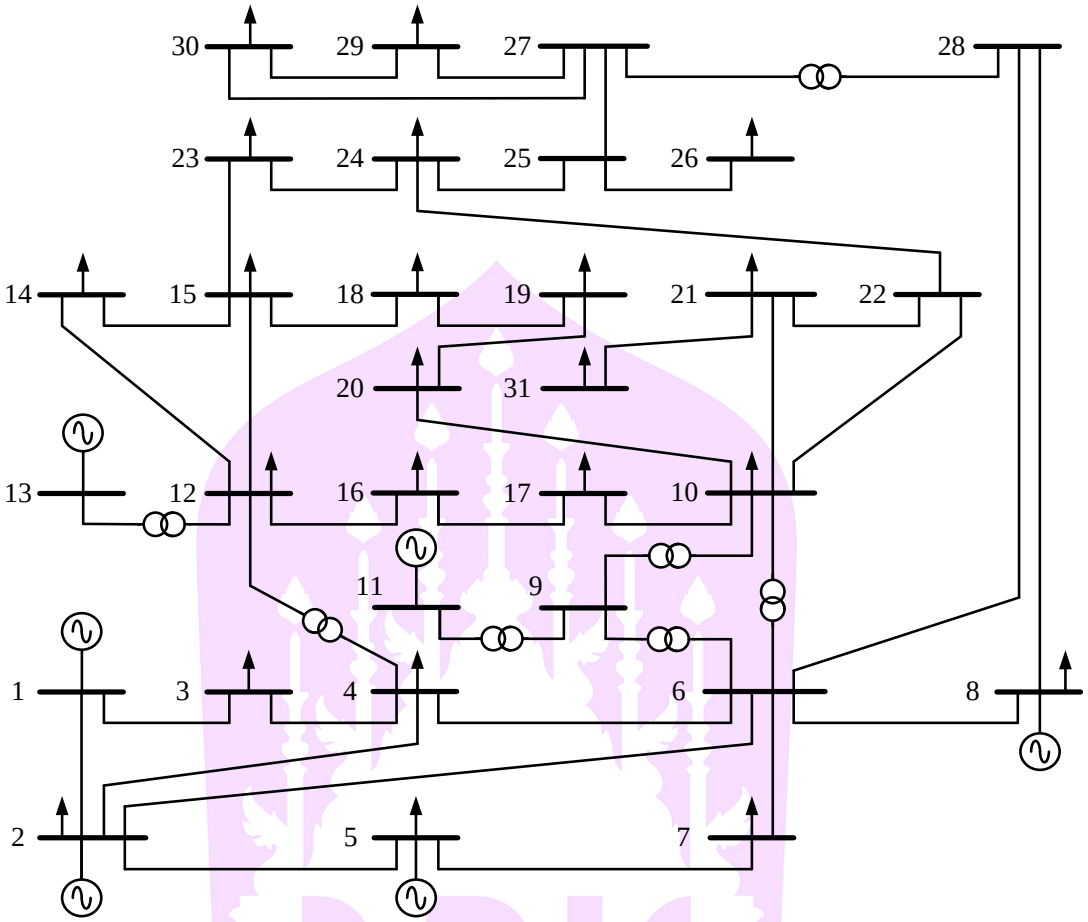

Figure 7 Single line diagram of IEEE 30 – bus system.

Three test cases are considered to verify the effectiveness of the proposed indices under various loading conditions.

Case 1: This case tests the load variation at a single load bus. Both real and reactive powers at bus 30 are increased until voltage collapse occurs.

Case 2: Both real and reactive powers at all load buses are increased until voltage collapse occurs.

Case 3: This is similar to case 2, however, single transmission lines' outage is also considered.

From the experimental results, it is found that the critical load scaling factors of case 1 and 2 are 3.0021 and 1.8721, respectively.

Table 1 LVSI and LAI for IEEE 30 – bus system

Line		Case 1 λ = 3.0021		Case 2 λ = 1.8721	
From	to	LVSI	LAI	LVSI	LAI
1	2	0.0979	0.1048	0.3753	0.4795
1	3	0.2465	0.0976	0.5762	0.2757
2	4	0.2126	0.0884	0.4287	0.1921
3	4	0.0574	0.0926	0.1679	0.2597
2	5	0.2056	0.0659	0.3910	0.1422
2	6	0.2880	0.1159	0.5379	0.2482
4	6	0.0935	0.1300	0.1794	0.2573
5	7	0.1277	0.0747	0.2573	0.1507
6	7	0.0296	0.0232	0.0384	0.0253
6	8	0.0793	0.1326	0.1444	0.2540
8	28	0.0194	0.0156	0.0811	0.0394
6	28	0.0610	0.0571	0.0729	0.0667
10	17	0.0217	0.3115	0.0751	0.7007
10	20	0.1018	0.3060	0.2555	0.7154
10	21	0.0072	0.1250	0.0770	0.7898
10	22	0.0252	0.2052	0.0448	0.6180
12	14	0.1223	0.2565	0.2397	0.5079
12	15	0.1169	0.4846	0.2408	1.0000
12	16	0.1534	0.4063	0.2145	0.5789
14	15	0.0060	0.0156	0.0023	0.0748
16	17	0.0978	0.2600	0.1126	0.3036
15	18	0.1662	0.3964	0.2436	0.5993
15	23	0.1292	0.2935	0.1034	0.4837
18	19	0.0681	0.2585	0.0874	0.3260
19	20	0.0217	0.2158	0.0715	0.5270
21	22	0.0317	0.4516	0.0404	0.8595
22	24	0.0443	0.2828	0.0570	0.5820
23	24	0.1770	0.3918	0.1549	0.3535
24	25	0.0779	0.2055	0.1592	0.2885

Table 1 (cont.) LVSI and LAI for IEEE 30 – bus system

Line		Case 1 λ = 3.0021		Case 2 λ = 1.8721	
From	to	LVSI	LAI	LVSI	LAI
25	26	0.1085	0.1804	0.2070	0.3514
25	27	0.0112	0.2582	0.2316	0.5198
27	29	0.4781	0.7546	0.3610	0.5375
27	30	0.7646	1.0000	0.5488	0.6154
29	30	0.4897	0.6383	0.2708	0.3262

Table 1 shows the LVSI and LAI obtained at the critical loading conditions of the IEEE 30 – bus system. It can be seen that line 27 – 30 and line 12 – 15 are the critical lines of cases 1 and 2, respectively, because their LAI are 1.0. A line with a high value of the LVSI can be considered as weak line in terms of the voltage stability. Such a line poses a risk of voltage instability for the connected buses, potentially leading to voltage instability issues. In addition, a line with a high value of the LAI can be considered as weak security line because its operating point may be near the thermal limit of the phase conductor.

Figures 8 and 9 show, for case 2, the variation of the LVSI and LAI of line 27 – 30 and line 12 – 15 under increasing of loads, respectively. From the results in Figure 8, it can be seen that the value of the LVSI rises to 1.0 when the voltage magnitude at bus 30 reaches the point of voltage collapse. However, because the LAI approaches 1.0 as the load scaling factor approaches 3.0, the maximum loading at bus 30 must be restricted to 3.0 times of base load. The results in Figure 9, also indicates that the value of LVSI of line 12 – 15 is less than 1.0. This implies that the voltage collapse condition cannot occur at both bus 12 and bus 15 in this test case. However, because the value of LAI is close to 1.0 when the load scaling factor closes to 1.870, the maximum loading is limited to 1.870 times of base load for case 2. This test result highlights the fact that increasing the load in power systems may be limited by transmission line security. The magnitude of the current flowing through the phase conductor may reach the current rating of the conductor before bus voltage collapse occurs.

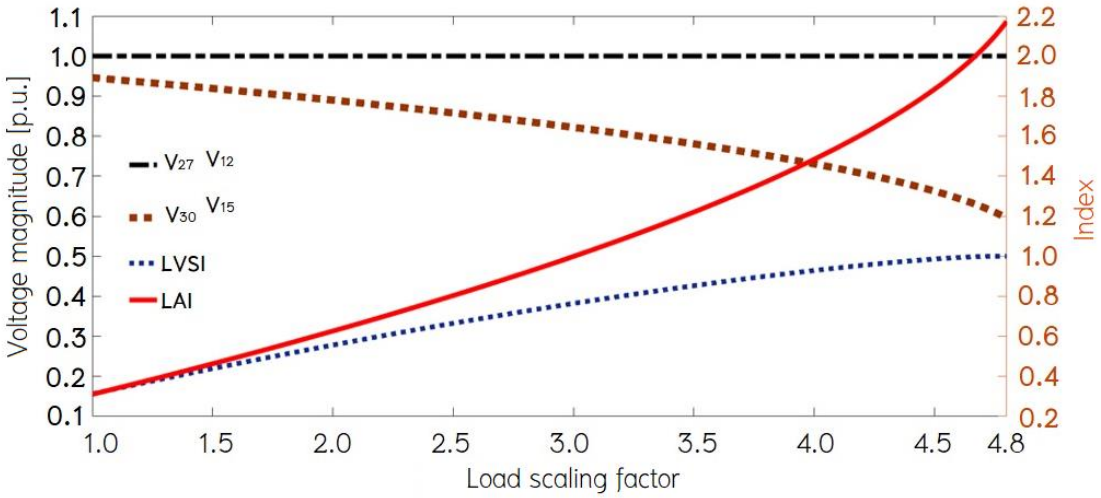

Figure 8 LVSI and LAI of line 27 – 30 for case 2.

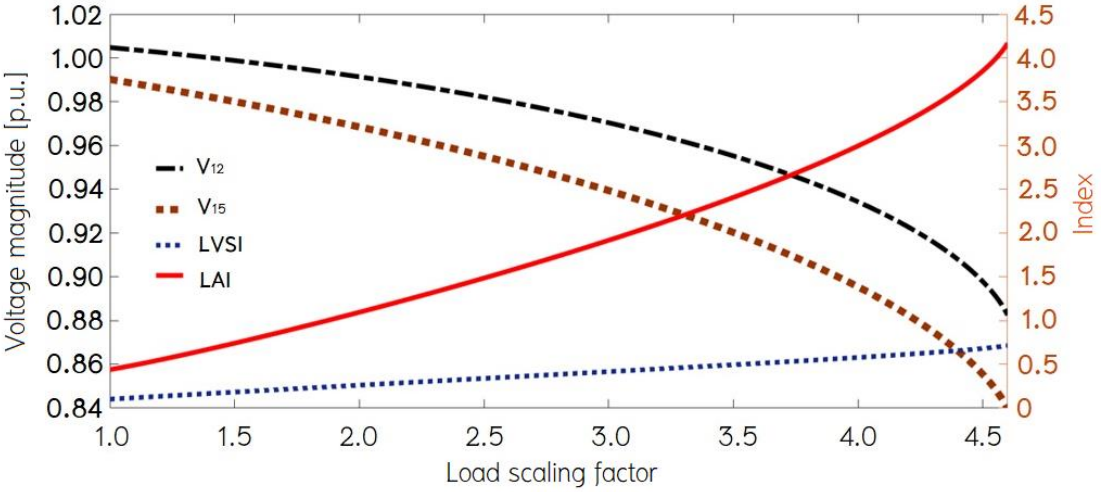

Figure 9 LVSI and LAI of line 12 – 15 for case 2.

For case 3, the results of the single line outage analysis of the IEEE 30 – bus system are summarized in Table 2. The maximum load scaling factor for the IEEE 30 – bus system under each line outage case is given. The critical lines in this test case are also identified based on the LAI, where the series current in phase conductor reaches its line ampacity before voltage collapse occurs. Nevertheless, in some case, a voltage collapse occurs before there is excess current in the transmission line.

Table 2 Maximum loading and critical line for IEEE 30 – bus system under line outage conditions

Line outage	λ_{max}	Critical line	LAI	LVSI
1 – 3	1.8949	12 – 15	1.0000	0.2413
12 – 15	1.0713	21 – 22	1.0000	0.0368
23 – 24	1.9098	10 – 21	1.0000	0.1011
27 – 29	1.4701	27 – 30	1.0000	0.7636

The results in Table 2 indicate that as the outage of line 27 – 29 happens, the LVSI of line 27 – 30 is high when system loading is increased. Hence, bus 30, which is a load bus, can be considered as a weak bus under this test condition.

Effect of Measurement Noise

The measured values of the bus voltage magnitude and real power flow obtained from each substation typically contain measurement noise. To investigate the influence of the measured values on the proposed indices, both real and reactive powers at all load buses are increased by 1. 80 time of the base load. In this study, even though the measured values used to determine the proposed indices can be obtained from both PMU and RTU devices, it is assumed that the measuring values are obtained solely from RTU devices.

The maximum uncertainties of the voltage magnitude and power flow measurements are assumed to be 0.4% and 1.0% of the reading, respectively. For each measurement, zero – mean Gaussian noise with a corresponding standard deviation is added. Testing has been performed using 5,000 Monte Carlo simulations.

From the experimental results in this test case, it is found that the largest LVSI occurs at line 1 – 3 while the largest LAI occurs at line 12 – 15.

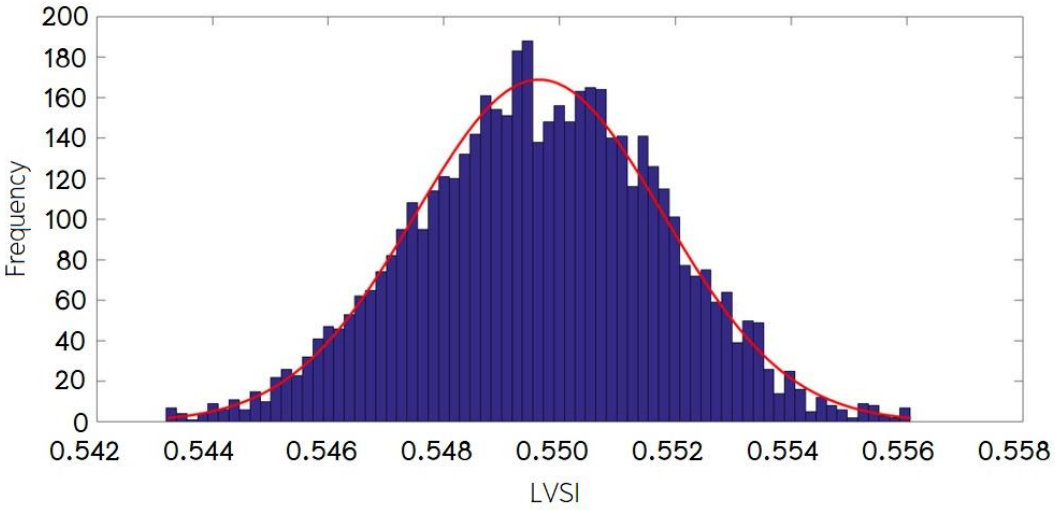

Figure 10 LVSI histogram of line 1 – 3 for IEEE 30 – bus system.

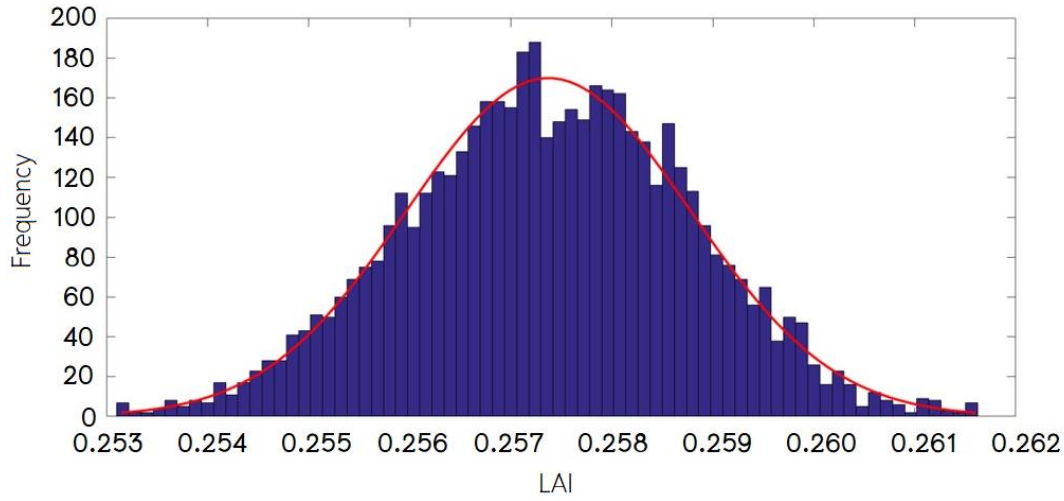

Figure 11 LAI histogram of line 1 – 3 for IEEE 30 – bus system.

Figures 10 and 11 show histograms of the LVSI and LAI computed using the measurements corresponding to line 1 – 3, respectively. Bus 1 is a generator bus, while the load bus 3 can be considered as a weak bus because its LVSI is greater than 0.50. However, the line 1 – 3 has a high security level since its LAI value is less than 0.30. The standard deviations of the LVSI and LAI obtained from line 1 – 3 are 0.19% and 0.27%, respectively.

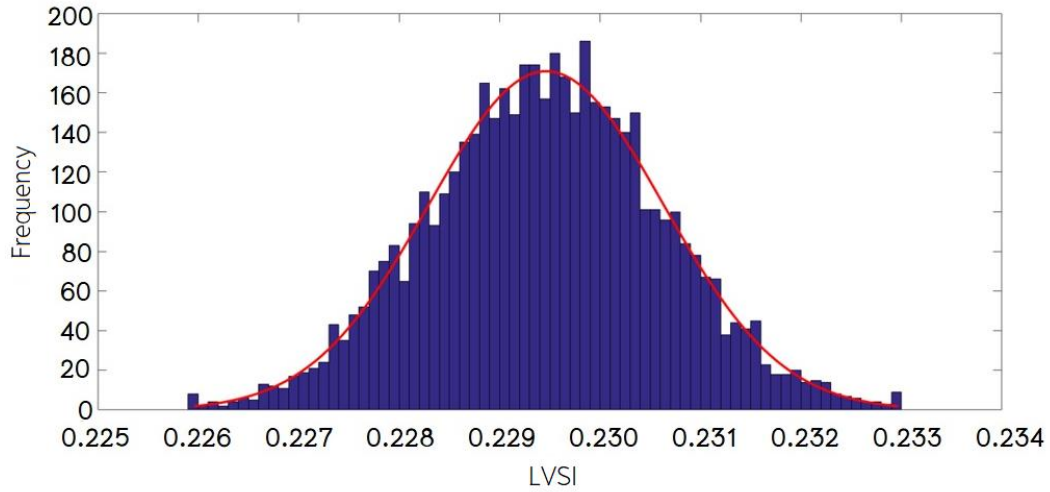

Figure 12 LVSI histogram of line 12 – 15 for IEEE 30 – bus system.

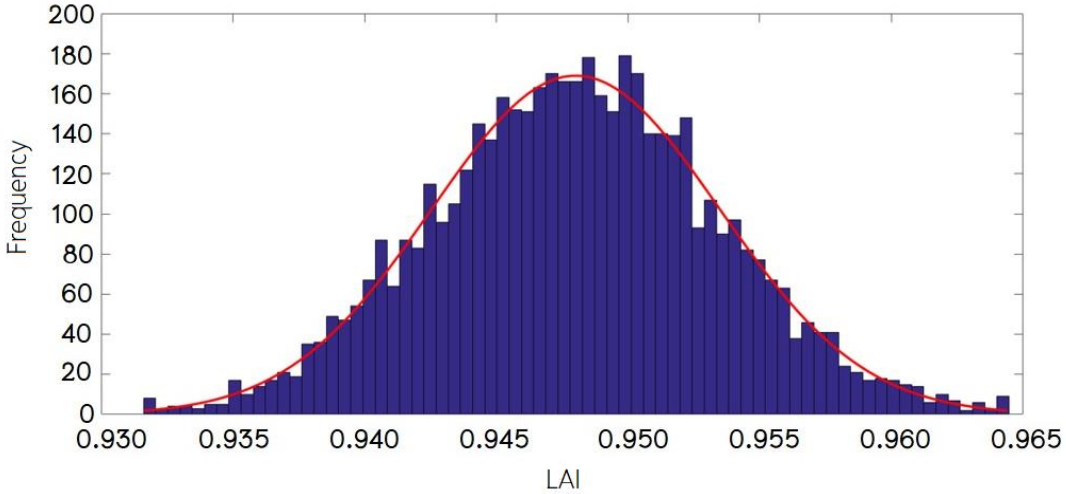

Figure 13 LAI histogram of line 12 – 15 for IEEE 30 – bus system.

Figures 12 and 13 show histograms of the LVSI and LAI of line 12 – 15 under this test condition, respectively. Bus 15 whose LVSI is less than 0.25 is a strong voltage bus, whereas bus 12 is a voltage – controlled bus. However, line 12 – 15 has a low security level because its LAI value is near unity. The standard deviations of LVSI and LAI for line 12 – 15 are 0.25% and 0.28%, respectively. It can be seen that the values of LVSI and LAI obtained using the conventional measurements have small percentage of standard

deviations. Consequently, the proposed indices can be applied to a real – time system to determine or monitor the voltage stability and security levels of each line.

Comparison with Other Voltage Stability Indices

In this subsection, the proposed LVSI has been compared with other voltage stability indices, that is, FVSI [3], Lmn [5], L_{QP} [44], and BVSI [9], under the loading conditions of the IEEE 30 – bus system. The testing conditions of case 1 and case 2 are used to validate the performance of the indices. The values of these LVSI must be less than 1.0 to maintain the voltage stability of the corresponding bus. Line 27 – 30 is a critical line and bus 30 is a weak bus for both test cases. The comparison results for case 1 and case 2 of the IEEE 30 – bus system are shown in Figures 14 and 15, respectively. It can be observed that the proposed LVSI and BVSI can successfully determine the point of voltage collapse. BVSI can provide voltage stability similar to that of the proposed LVSI. Nevertheless, since different phase voltages between the sending and receiving buses are also required to compute BVSI, PMU measurements are required. By contrast, FVSI, Lmn, and L_{QP} fail to identify the collapse point. In Case 1, voltage collapse occurs before the values of FVSI, Lmn, and L_{QP} are close to 1.0. In Case 2, voltage collapse occurs before the values of FVSI and Lmn are close to 1.0, whereas the L_{QP} value is 1.0 before voltage collapse occurs.

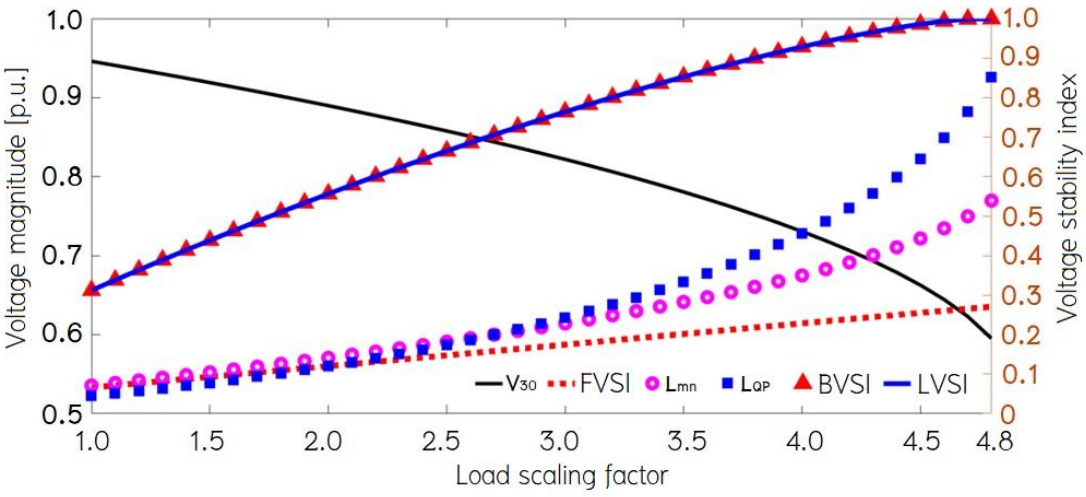

Figure 14 Comparison of various voltage stability indices of line 27 – 30 for IEEE 30 – bus system (case 1).

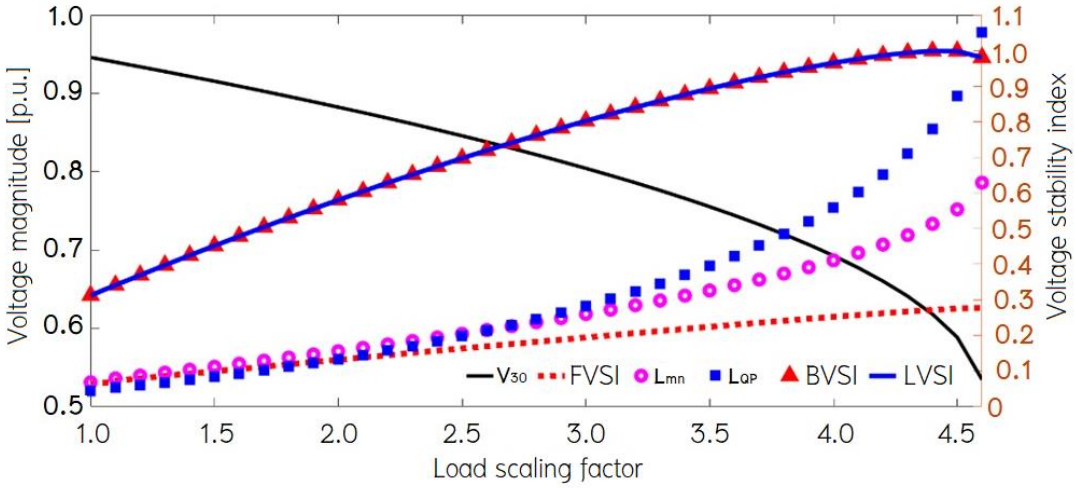

Figure 15 Comparison of various voltage stability indices of line 27 – 30 for IEEE 30 – bus system (case 2).

Conclusion

Two indices which is LVSI and LAI have been proposed in this Chapter. The indices are derived based on real power flow and real power loss of a transmission line. A technique based on a quadratic equation to estimate phase angle difference has been provided to avoid phase angle measurements. Therefore, the proposed indices use only bus voltage magnitudes and real power flow measurements obtained from common RTUs to assess the voltage stability and line security states of power systems under different operating conditions. The results for small and large power networks show that the proposed LVSI can determine the voltage collapse point and weak buses whereas the proposed LAI can determine the critical and weak security lines.

Chapter III

Thermal Modelling of Power Components

This chapter studies the power components of power systems such as the transmission line and the power transformer. Considering the thermal states using environmental temperature and characteristics conductor of the overhead transmission line [45]. According to IEEE standard 738 – 2012, the heat balance equation can calculate the conductor temperature by considering ambient temperature, wind speed, wind direction, and solar radiation.

The power transformer in this study [46 – 48] is an oil immersed transformer that has a cooling system for the transformer. The thermal in the transformer, caused by internal conditions such as load flow in the transmission line in to winding of transformer. External conditions such as ambient temperatures, wind speed, wind direction, and solar radiation affect the heat dissipation in the transformer. The top – oil and the hot – spot winding temperature are important factors in determining the transformer thermal rate [49 – 52], calculation according to IEEE C57.91 – 2012. Therefore, in this chapter, the thermal equations of the state of the transmission line and the power transformer are developed, considering the conductor temperature, the top oil and the hot – spot winding temperatures.

Transmission Line

The temperature of conductors in the transmission line varies according to the environmental conditions surrounding the conductor and exhibits a temperature change proportional to the amount of current flowing through the transmission line. When calculating the power flow to match the actual operating conditions of the power system, it is analyzed whether the power transmission is adequate to meet the electrical load requirements. This analysis of the power flow and power loss values in the transmission line ensures that they match the actual losses. This precision is essential for planning an appropriate and safe power distribution strategy.

According to the IEEE standard 738 – 2012. The effective value [8, 53, 54]. of a steady – state current phasor flowing through the conductor, can be calculated by using the following heat balance equation

$$I_{C,eff} = \sqrt{\frac{q_c + q_r - q_s}{R(T_c)}} \tag{19}$$

where q_c is the heat loss due to convection,

q_r is heat due to radiation,

q_s is the heat gain from the sun,

$R(T_c)$ is AC resistance per unit length of conductor which is a function of conductor temperature.

Weather condition and a conductor's physical properties [40] can be calculated by

$$q_c = f_{qc}(\psi) \tag{20}$$

where $\psi = \begin{bmatrix} Ta & w_d & w_s & Q_s \end{bmatrix}^T$ denotes the vector containing weather environment parameters,

w_d is direction of wind in radian,

w_s is speed of wind in m/s,

Q_s is the elevated corrected total solar and sky radiated heat flux rate.

$$q_r = 0.0178D \in \frac{(T_c + 273)^4 - (T_a + 273)^4}{100^4} \tag{21}$$

where T_c is the conductor temperature in $^{\circ}C$,

T_a is the ambient temperature in $^{\circ}C$,

D stands for the conductor diameter in m,

$\in$ is emissivity.

$$q_s = \lambda Q_s \sin(\theta) A' \tag{22}$$

where λ is the solar absorptivity,

A' is the projected area of conductor per unit length,

θ is a solar radiation angle corresponding to the solar altitude and the azimuth angle of sun.

The AC resistance and reactance of transmission line per unit length of conductor and conductor temperature [15], can be expressed as

$$R(T_c) = R_0 \left(1 + \alpha_R (T_c - T_0)\right) \tag{23}$$

where R_0 is AC resistance per unit length at the reference temperature of T_0,

$R(T_c)$ is AC resistance per unit length at the reference temperature of T_c,

α_R is the line resistance's temperature coefficient.

Power Transformer

A power transformer is a crucial component in an electrical power system. Its primary function is to convert voltage levels, both increasing voltage for transmission in the power system and reducing voltage for distribution to users. By stepping up the voltage for transmission, the power transformer minimizes energy losses during power transmission through the network. Conversely, stepping down the voltage before distribution ensures that electricity is delivered to users at an appropriate and safe voltage level.

Power transformers play a continuous role in managing voltage levels within an electrical system. One key aspect of their operation is the dissipation of heat. Efficient heat dissipation is essential to ensure the safe and effective functioning of the power transformer. It helps maintain optimal operating conditions and prevents overheating, contributing to the overall reliability of the electrical power system.

Selecting an appropriate method for heat dissipation is crucial for the efficient and safe operation of power transformers. Effective heat dissipation ensures that the transformer operates efficiently and remains safe over an extended period. Oil cooling involves using oil as a heat transfer medium in the power transformer. Oil has excellent heat dissipation capabilities, allowing the transformer to operate for extended periods without degradation. The oil is typically stored in a tank or surrounding the transformer. Air Cooling of power transformers may incorporate air cooling systems using fans or designed air vents to expel heat to the external environment. Water Cooling, in certain cases, water can be utilized as a heat transfer medium in the transformer's cooling process. Water is introduced into the cooling system and directed through pipes or channels for efficient heat dissipation.

Generally, oil immersed transformers [55, 56] are the transformer with its winding and core are immersed in the mineral oil, which has good electrical insulating property to block the current flow through the oil and high thermal conductivity. This method can be divided into four types

Oil Natural Air Natural (ONAN): This cooling method may be used for transformers up to about 30 MVA. In this method, the heat generated in the core and winding is transferred to the oil. The heated oil moves in an upward direction and flows from the upper portion of the transformer tank according to the principle of convection. The heat from the oil will dissipate into the atmosphere due to the natural air flow around the transformer. In this case, the oil in the transformer will keep circulating because of natural convection and will dissipate heat into the atmosphere due to natural conduction.

Oil Natural Air Forced (ONAF): generally, this method of transformer cooling is useful for large transformers up to about 60 MVA. Heat dissipation can be improved by applying forced air to the dissipating surface. The heat dissipation rate is faster and higher in the ONAF transformer cooling method than in the in the ONAN cooling system. In this manner, fans are mounted near the radiator and can be provided with an automatic starting arrangement that turns on when the temperature increases beyond a certain value.

Oil – Forced Air – Forced (OFAF): cooling methods are provided for higher – rated transformers at substations or power stations. In this method, oil is circulated with the help of a pump, and then compressed air is forced to pass through the heat exchanger with the help of high – speed fans. Furthermore, the heat exchangers can be mounted separately from the transformer tank and connected through pipes at the top and bottom.

Oil – Forced Water – Forced (OFWF): occurs when the ambient temperature of water is much lower than that of atmospheric air in the same weather condition, water may be used as a better heat exchange medium than air. The oil is forced to flow through the heat exchanger with the help of a pump, where the heat is dissipated in the water, which is also forced to flow. The heated water is taken away to cool in separate coolers.

Like every existing machine, [57, 58] transformers cannot work without energy losses. The transformer has no moving parts, so the mechanical losses are absent. Transformer losses are classified as no – load losses and load losses. These types of losses are common to all types of transformers, regardless of transformer application or power rating. However, there are two other types of losses: extra losses created by the non – ideal quality of power and auxiliary or cooling losses, which may apply particularly to larger transformers and are caused by the use of cooling equipment such as fans and pumps.

Exponents for Temperature Rise Equations

The exponent of the temperature rise used in the calculations assists in addressing the variation in the temperature changes of the transformer over different time periods. This allows for adjustments based on the operational conditions and heat dissipation characteristics inherent to the power transformer. In the context of the equation for determining the temperature in a power transformer, the exponent of the temperature increase may vary according to the transformer's operating conditions and its inherent heat dissipation characteristics. Generally, the exponent used in the calculations, known as the exponent of temperature rise, is adaptable to the specific working conditions and heat dissipation characteristics of the power transformer. The suggested exponents for use in the temperature – rise equations are given the effect on the transformer [59]. Working on

the load at all times is heating, resulting in loss of life to the transformer. The critical heat point is the high heat point that causes the transformer insulation to deteriorate prematurely. The insulation life or insulation deterioration depends on the temperature of the transformers. According to the IEEE Standard, C57.91 [60, 61]. The calculation method for oil temperature considering load variation in power transformers, particularly when subjected to varying loads, involves utilizing computational methods with specified parameters denoted as m and n. These parameters can be estimated from the load variation, and the calculation process is outlined based on the heat – dissipation characteristics of the transformer.

Table 3 Exponents of power transformer

Type of cooling	m	n
Oil Natural Air Natural (ONAN)	0.8	0.8
Oil Natural Air Force (ONAF)	0.8	0.9
Oil Forced Air Forced (OFAF)	0.8	0.9
Oil Forced Water Forced (OFWF)	0.8	0.9
Oil Directed Air Forced (ODAF)	1.0	1.0
Oil Directed Water Forced (ODWF)	1.0	1.0

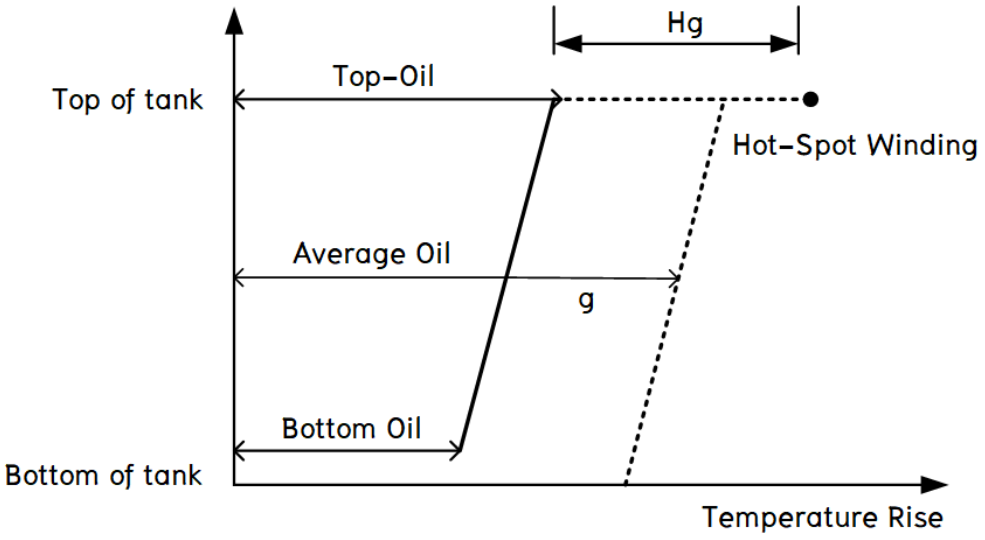

Figure 16 Heat diagram of mineral – oil immersed transformers.

Hot – Spot Winding Temperature

The hot – spot winding has been the highest temperature area in the transformer based on flux leakage from the windings and can degrade the insulating paper making the transformer susceptible to failure. Since transformer life is dependent on the insulating paper, accurately monitoring temperature conditions is critical. The hot – spot winding temperature in a transformer winding is the sum of three components, the ambient temperature rise, the top – oil temperature rise, and the hot – spot winding temperature rise over the top – oil temperature.

During a transient period, the hot – spot winding temperature rise over the top – oil temperature varies instantaneously with transformer loading, independently of time [7, 62, 63]. The variation of the top – oil temperature is described by an exponential equation based on oil time constant.

The hot – spot winding temperature is assumed to consist of three components given by the following equation:

$$\Theta_H = \Theta_A + \Delta\Theta_{TO} + \Delta\Theta_H \tag{24}$$

where Θ_H is the winding hot – spot winding temperature, $^\circ C$,

Θ_A is the average ambient temperature during the load cycle, $^\circ C$,

$\Delta\Theta_{TO}$ is the top – oil rise over ambient temperature, $^\circ C$,

$\Delta\Theta_H$ is the winding hot – spot winding rise over top – oil temperature, $^\circ C$.

Top – Oil Temperature

The top – oil temperature rise at a time after a step load change is given by the following exponential expression containing an oil time constant [64]. The top – oil temperature is given by the following equation

$$\Theta_{TO} = \Theta_A + \Delta\Theta_{TO} \tag{25}$$

$$\Delta\Theta_{TO} = \Theta_{TO} - \Theta_A \tag{26}$$

$$\Delta\Theta_{TO} = \left(\Delta\Theta_{TO,U} - \Delta\Theta_{TO,i}\right)\left[1 - \exp^{-\frac{t}{\tau_{TO}}}\right] + \Delta\Theta_{TO,i} \quad (27)$$

where Θ_{TO} is the top – oil temperature, $^{\circ}C$,

$\Delta\Theta_{TO,U}$ is the ultimate top – oil rise over ambient temperature, $^{\circ}C$,

$\Delta\Theta_{TO,i}$ is the initial top – oil rise over ambient temperature for t=0, $^{\circ}C$,

t is duration of load, hour,

τ_{TO} is the oil time constant of top – oil rise and the initial top – oil rise, hour.

The transient hot – spot winding temperature rise over top – oil temperature is given by

$$\Delta\Theta_{H} = \left(\Delta\Theta_{H,U} - \Delta\Theta_{H,i}\right)\left[1 - \exp^{-\frac{t}{\tau_{w}}}\right] + \Delta\Theta_{H,i} \quad (28)$$

where $\Delta\Theta_{H,U}$ is the ultimate hot – spot winding rise over top – oil temperature for load L, $^{\circ}C$,

$\Delta\Theta_{H,i}$ is the initial hot – spot winding rise over top – oil temperature for t=0, $^{\circ}C$,

τ_{w} is the winding time constant at hot – spot location, hour.

For the two – step overload cycle with a constant equivalent prior load the initial top – oil rise is given by the following:

$$\Delta\Theta_{TO,i} = \Delta\Theta_{TO,R}\left[\frac{K_i^2 R + 1}{R + 1}\right]^n \quad (29)$$

For the multi – step load cycle analysis with a series of short – time intervals, Equation is used for each load step, and the top – oil rise calculated for the end of

the previous load step is used as the initial top – oil rise for the next load step calculation. The ultimate top – oil rise is given by the following equation:

$$\Delta\Theta_{TO,U} = \Delta\Theta_{TO,R}\left[\frac{K_U^2 R + 1}{R + 1}\right]^n \quad (30)$$

The initial hot – spot winding rise over top – oil is given by

$$\Delta\Theta_{H,i} = \Delta\Theta_{H,R} K_i^{2m} \quad (31)$$

The ultimate hot – spot winding rise over top – oil is given by

$$\Delta\Theta_{H,U} = \Delta\Theta_{H,R} K_U^{2m} \quad (32)$$

Time constant at rated load

$$\tau_{TO,R} = \frac{C\Delta\Theta_{TO,R}}{P_{T,R}} \quad (33)$$

where $\tau_{TO,R}$ is the time constant for rated load beginning with initial top – oil temperature rise of 0 °C, hour,

$\Delta\Theta_{TO,R}$ is the top – oil rise over ambient temperature at rated load on the tap position to be studied, $^{\circ}C$,

K is the ratio of load to rated load, per unit ,

C is the thermal capacity of the transformer, W–h / $^{\circ}C$,

$P_{T,R}$ is the total loss at rated load, Watt,

R Is the ratio of load loss at rated load to no – load loss on the tap position to be studied.

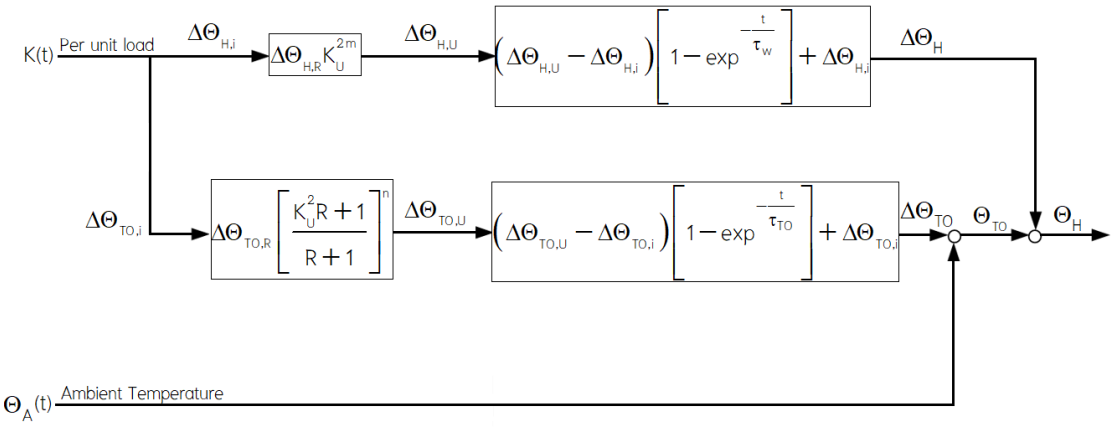

Figure 17 Thermal diagram of power transformer.

Thermal model is a component of the IEEE C57.91 which is a standard related to the design and testing of power transformers, thermal modeling of power transformers within this standard may constitute a section or part that outlines the specifications regarding the thermal model of power transformers under various operating conditions. It encompasses calculations for the hot – spot winding temperature and the top – oil temperature, which serves as the heat – producing medium within the power transformer.

The power transformer may operate at temperatures exceeding 110 °C for brief periods. This heat accumulation process allows for the safe accumulation of heat above the hot – spot winding temperature under various conditions, without adversely affecting the normal lifespan of the power transformer. The equation provided in IEEE C57.91 is employed to calculate the maximum hot – spot winding temperature and the top – oil temperature as a function of the transformer's operational loss of life. A discrete thermal model transformer refers to a non – continuous temperature model of a power transformer that uses temperature values divided into discrete parts. These parts are not continuous and can be divided into intervals or discrete points to gather information about the temperature of the transformer at different time intervals or under specified conditions.

Thermal State Estimation Equations

This section presents the thermal states estimation equations developed from the thermal model for transmission lines and power transformers. These equations are utilized to estimate the thermal states of the power system, considering the heat conductor of the transmission lines, including the top – oil and the hot – spot winding temperature of the power transformers.

Conductor Temperature of Transmission Line

The calculation of the overhead transmission line thermal model utilizes mathematical equations that depict the relationship between heat generated in the transmission line and environmental conditions. These equations are developed from assessing heat values, which can be calculated by considering the environmental temperature, heat conducted through the transmission line, and heat dissipated by the transmission line. The mathematical equations used in the model are derived from principles of heat transfer and thermal conduction and can be tested by estimation from experimental data or analytical methods. Developing an accurate model to calculate the temperature of the transmission line during power flow and load conditions is essential for planning and operating electrical systems. Generally, temperature – dependent parameters of the transmission line are used in the thermal model to calculate the temperature of the transmission line at specified time intervals. This model calculates the temperature and thermal state of the transmission line at various points, considering different factors that impact heat loss, such as changing environmental temperatures, and heat dissipation through the surrounding air. The equation used to calculate the temperature of the conductor can be defined as follows, subtracting the sum of the heat loss due to convection and radiation, then dividing by the resistance per unit length of the conductor, which is a function of the conductor. The conductor temperature of line can be estimated using the equation (34) which has to be included into the state estimation problem explained in Chapter 4.

$$I^2 - \left(\frac{q_c + q_r - q_s}{R(T_c)} \right) = 0 \tag{34}$$

The temperature of the power transformer changes according to the load currents, and the temperature change cannot occur rapidly owing to the temperature of the environment and the heat dissipation of the transformer, which are factors in the temperature control. However, when estimating the top – oil and the hot – spot winding temperatures, the time period in which the load curve changed had different values. Therefore, the transformer temperature during the loading period can be calculated using the following equation

Top – Oil Temperature of Power Transformer

A discrete thermal model allows for the analysis of temperature behavior based on various conditions. The equation used to calculate the discrete thermal model of the top – oil temperature [65, 66] is given by

$$\Theta_{TO}(k)=\frac{\tau_{TO}}{\tau_{TO}+\Delta t}\Theta_{TO}(k-1)+\frac{\tau_{TO}}{\tau_{TO}+\Delta t}\left[\left[\frac{I^2(k)R+1}{R+1}\right]^n\Delta\Theta_{TO,R}+\Theta_A\right] \quad (35)$$

where Δt is the time change between any sampling period, minute,

I is operating current / ratted current, A,

k is the time step.

Hot – Spot Winding Temperature of Power Transformer

The temperature of the hot – spot at the winding inside the power transformer varies according to the top – oil temperature, the winding time constant at the hot – spot location will be used in this equation, from the discrete thermal model of the top – oil temperature (35) can calculation the discrete thermal model of the hot – spot winding temperature [67] is given by

$$\Theta_H(k)=\left(\frac{\Delta t}{\Delta t+\tau_w}\right)\Theta_{TO}(k)+\left(\frac{\tau_w}{\Delta t+\tau_w}\right)\Theta_H(k-1)+\left(\frac{\Delta t}{\Delta t+\tau_w}\right)\Delta\Theta_{HR}\left(I-(k)\right)^{2m} \quad (36)$$

Simulation Results

This section presents the simulation of the proposed thermal states estimation equations by simulating the overhead transmission line, the top – oil temperature, and the hot – spot winding temperature.

Case of Transmission Line

The simulation testing of the thermal model for the conductor employed parameters obtained from the conductor datasheet, specifically for the aluminum conductor steel reinforced (ACSR) type named GOAT. The simulation utilized data from [68], the wind speed is 0.80 m/s, the angle between the wind direction and the conductor axis is 90° and ambient temperature is 40° C. Tested at various levels of irradiance from 400 to a maximum of 1000 W/m^2, tested included current values in the transmission line ranging from 50 to 700 A. The results of the overhead transmission line are as shown in Figure 18. If the current magnitude is specified, the temperature of the conductor can be calculated at any irradiance level. The higher the current magnitude, the higher the temperature of the conductor, even under similar ambient temperature conditions. Moreover, if the irradiance increases, it will also affect the temperature of the conductor.

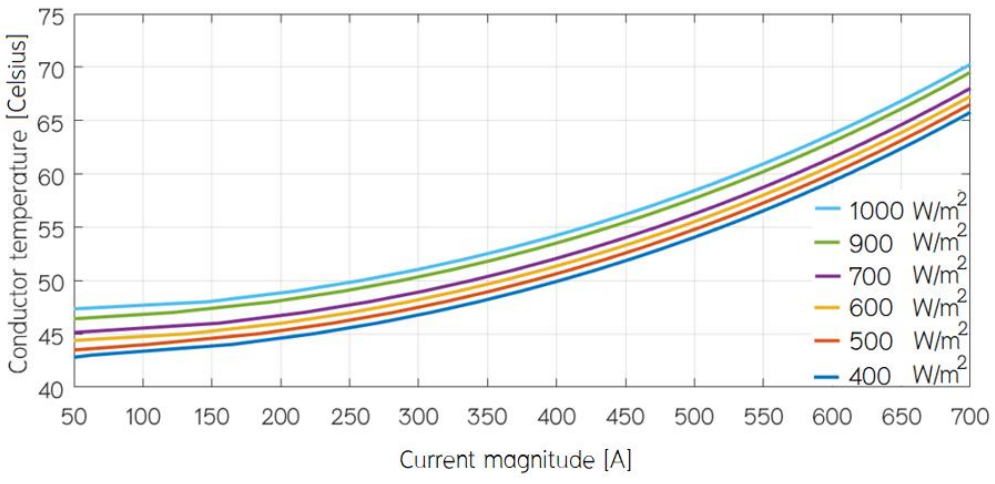

Figure 18 Relationship between current magnitude and conductor temperature.

Case of Power Transformer

In this section describes the simulation of the proposed thermal power transformer model simulating the top – oil and the hot – spot winding temperatures. The testing was conducted on two case studies of power transformers rated at 25 and 250 MVA. Physical data and thermal conductivity data were utilized for the experimentation.

Case 1: 25 MVA power transformer

The modeling using data of transformer 25 MVA, 66/11 kV ONAF cooling transformer, the obtainable weather and load data are utilized for calculating the hot – spot winding temperature and the top – oil temperature models were tested under various load currents [16], based on IEEE standard C57.91 – 2011. The load values are as follows Figure 19. The top – oil temperature and the hot – spot winding temperature models were tested under various load currents with different load values over varying durations of operation. The ambient temperature considered in this calculation to study assume at 28 $^{\circ}$C the effect of changing load levels on the transformer data of the testing thermal model is as follows:

Table 4 Data of transformer 25 MVA

Rated data		Temperature data	
Power	25 MVA	Type of cooling (m, n) ONAF	0.8, 0.9
Voltage	66 kV	Ratio of load loss at rated load to no load loss (R)	5
Winding I^2R losses	57,390 W	Top – oil rise over ambient at rated load ($\Delta\Theta_{TO,R}$)	38.3 $^{\circ}$C
Winding eddy losses	10,690 W	Hot – spot rise over top – oil at rated load ($\Delta\Theta_{HS,R}$)	23.5 $^{\circ}$C
Stray losses	32,393 W	Ambient temperature ($\Delta\Theta_{HS,R}$)	28.0 $^{\circ}$C
Core losses	0 W		
Weight of oil	10,800 kg		

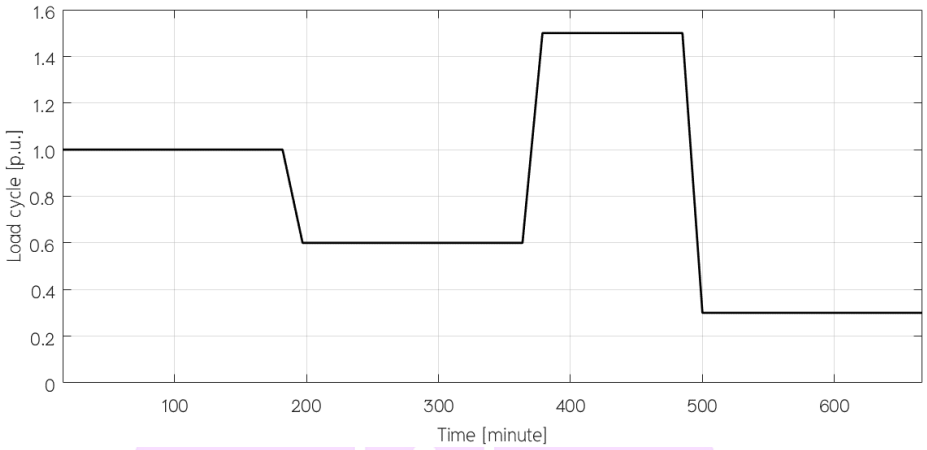

Figure 19 Load cycle of thermal model test power transformer.

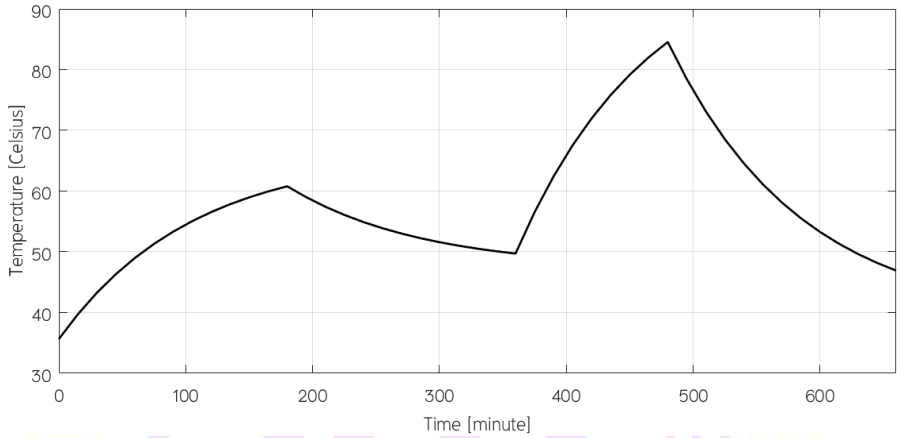

Figure 20 The top – oil temperature of transformer 25 MVA.

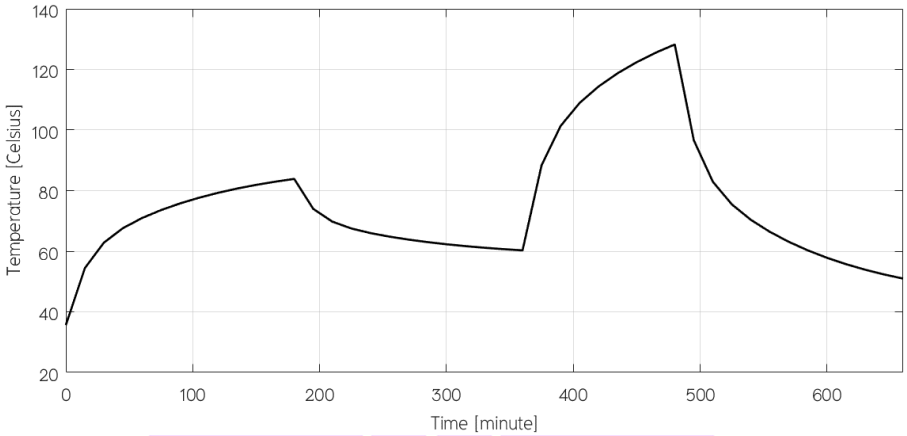

Figure 21 The hot – spot winding temperature of transformer 25 MVA.

Figure 20, the top – oil temperature is calculated using the equation for top – oil rise over ambient at rated load, considering an ambient temperature of 28 °C. Therefore, the top – oil temperature starts at 35 °C and increases when the load value is 1 p.u. From the calculations. The maximum top – oil temperature is 85 °C, when the load reaches a maximum of 1.5 p.u.

Figure 21, the calculation starts at hot – spot rise over top – oil at rated load, resulting in an initial value 38.3 °C. The maximum hot – spot winding temperature is 128 °C. when the load reaches a maximum of 1.5 p.u.

Case 2: 250 MVA power transformer

Modeling using data from transformer 250 MVA [68, 69], the load values as shown in Figure 19. The top – oil and the hot – spot winding temperatures models were tested under various load currents with different load values over varying operation durations. The ambient temperature considered in this calculation to study assume at 28 °C the effect of changing load levels on the transformer data of the testing thermal model is as follows:

Table 5 Data of transformer 250 MVA

Rated data		Temperature data	
Power	250 MVA	Type of cooling (m, n)	0.8, 0.9
		ONAF	
Voltage	118 kV	Ratio of load loss at rated load to no load loss (R)	6
Winding I^2R losses	411,780 W	Top – oil rise over ambient at rated load ($\Delta\Theta_{TO,R}$)	38.3 °C
Winding eddy losses	29,469 W	Hot – spot rise over top – oil at rated load ($\Delta\Theta_{HS,R}$)	20.3 °C
Stray losses	43,391 W	Ambient temperature ($\Delta\Theta_{HS,R}$)	28.0 °C
Core losses	0 W		
Weight of oil	73,887 kg		

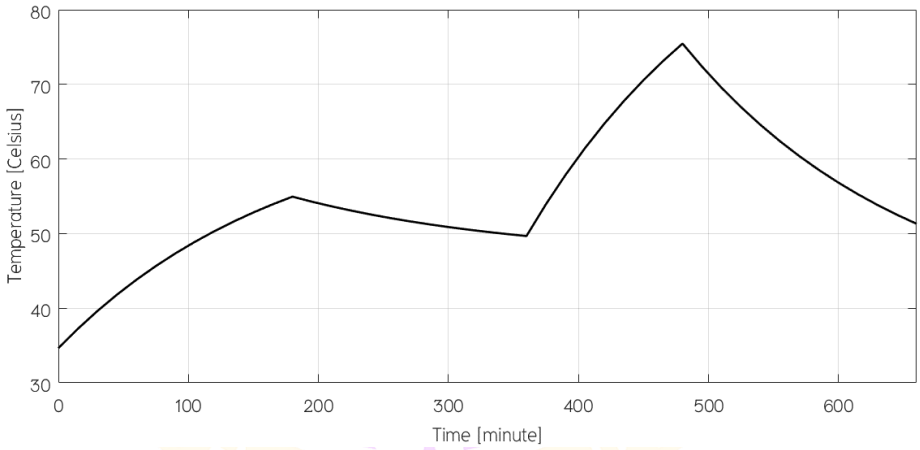

Figure 22 The top – oil temperature of transformer 250 MVA.

Figure 22, the top – oil temperature starts at 35 °C and increases when the load value is 1 p.u. From the calculations, the maximum top – oil temperature is 75 °C, when the load reaches a maximum of 1.5 p.u.

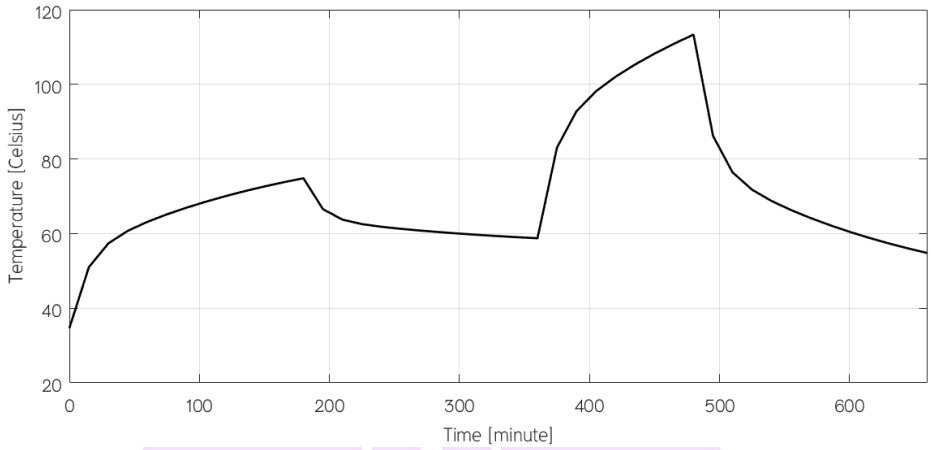

Figure 23 The hot – spot winding temperature of transformer 250 MVA.

Figure 23, the hot – spot winding temperature exhibits a similar pattern to the top – oil temperature, but the calculation starts at hot – spot rise over top – oil at rated load, resulting in an initial value 38.3 $^{\circ}$C. From the calculations, the maximum hot – spot winding temperature is 115 $^{\circ}$C, when the load reaches a maximum of 1.5 p.u.

Conclusion

The thermal state of the transmission line is the conductor temperature while the thermal states of the power transformer are the top – oil and the hot – spot winding temperatures. The mathematical models of the power components corresponding to those thermal states have been explained in this chapter. The thermal state estimation equations which can be applied to the state estimation problem have also been given, and some simulation testing has been performed. The steady – state thermal model of the transmission line is used because its thermal time constant is quite small. However, the discrete – time thermal equations of the power transformer are used to calculate the top – oil and the hot – spot winding temperatures due to the steady – state thermal time constants of the oil and the winding of the transformer are usually large.

Chapter IV

State Estimation Algorithm

Problem Formulation

The temperature – dependent state estimation in a three – phase network, where tap and admittance parameters of transformers are also the state variables, can be formulated as the following nonlinear constrained optimization problem based on the weighted least square (WLS) criterion:

$$\left.\begin{aligned} &\phi = \min \frac{1}{2} r^{T} W r, \\ &\text{s.t.} \quad r = z - h(\nu, t), \\ &f(\nu, t) \leq 0, \\ &g(\nu, t) = 0, \\ &\nu_{min} \leq \nu \leq \nu_{max}, t_{min} \leq t \leq t_{max}, \end{aligned}\right\} \tag{37}$$

where r represents for the residual vector, W is a diagonal weight matrix containing the corresponding standard deviation of each measurement, z denotes the measurement vector, $h(\cdot)$ is the measurement function, $f(\cdot)$ and $g(\cdot)$ are the inequality and equality constraints, respectively. The state variables $x = (\nu, t)$ consists of $\nu = (V_{abc}, \theta_{abc})$, a vector of magnitude and phase angle of the three – phase voltage phasor at each bus, and t, a vector containing transformer tap, a_t, leakage reactance of transformer, x_t, line conductor temperature, To, and weather related variables. The following weather variables, i.e. Ta, ambient temperature, ws, wind speed, wd, wind direction, and Qs, solar heat flux rate are considered in this formulation. They are required in computing the heat – balance condition of each overhead transmission line. The weather parameters are assumed to be available and can be obtained from meteorological data. Therefore, $t = (a_t, x_t, To, Ta, ws, wd, Qs)$.

The measurement function is composed of,

$$h(v,t) = (h_{Pmu}, h_{Rtu}, h_{Wea}) \tag{38}$$

where h_{Pmu} is the measurement function for the PMUs. It consists of bus voltage and current phasors measured in polar coordinate. In this work, a rectangular coordinate of current phasor is used as measured value. The standard uncertainty of the current phasor in the rectangular coordinate is computed using the uncertainty propagation approach [70]. h_{Rtu} is the measurement function for the RTUs. It consists of the bus voltage magnitude, the power injection, and the power flow measurement functions. And h_{Wea} is weather related measurements. Accordingly, the measurement vector z comprises the data obtained from the corresponding measuring devices;

$$z = (z_{Pmu}, z_{Rtu}, z_{Wea}) \tag{39}$$

The inequality constraint consists of

$$f(v,t) = (f_{Vm}, f_{Tr}, f_{Hb}, f_{Wea}) \tag{40}$$

where f_{Vm} is obtained from the bus voltage magnitude constraints, f_{Tr} contains inequality related to transformer parameters, f_{Hb} denotes inequality constraints derived from heat – balance conditions, i.e. equation. (19) in Chapter 3, and f_{Wea} contains inequality related to weather parameters, e.g. To ≥ Ta. For the equality constraint, three sub – constraints can be grouped as follows;

$$g(v,t) = (g_{Vref}, g_{Zinj}, g_{Hb}) \tag{41}$$

where g_{Vref} is obtained from reference bus voltage phasor constraints, g_{Zinj} represents zero injection constraints, and g_{Hb} denotes equality constraints derived from heat – balance conditions of each line where its conductor temperature is estimated, i.e. equation. (34).

Solving Solution

By introducing the nonnegative slack variable vectors $(s \geq 0)$ into inequality constraints in (37) and including the slack variables in the logarithmic barrier terms of the objective function. The (37) can be transformed into the equation (42).

$$\begin{aligned} \text{Minimize} \quad & \frac{1}{2} r^T R^{-1} r - \mu \sum_{i=1}^{p} \ln s_i, \\ \text{Subject to} \quad & \begin{cases} r - z + h(x) = 0, \\ g(x) = 0, \\ f(x) + s = 0, \end{cases} \end{aligned} \tag{42}$$

where s_i is the ith element of s, p is the number of rows of f(x), $\mu > 0$ is the barrier parameter. The parameter μ closes to zero when the solution is found.

The Lagrangian function of the problem (42) can be defined as

$$L = \frac{1}{2} r^T R^{-1} r - \mu \sum_{i=1}^{p} \ln s_i - \lambda^T [f(X) + s] - \rho^T g(x) - \pi^T [r - z + h(x)] \tag{43}$$

Karush–Kuhn–Tucker conditions are provided by

$$0 = \mu e + \Lambda s, \tag{44}$$

$$0 = f(x) + s, \tag{45}$$

$$0 = g(x), \tag{46}$$

$$0 = r - z + h(x), \tag{47}$$

$$0 = r - R\pi, \tag{48}$$

$$0 = F^T \lambda + G^T \rho + H^T \pi, \tag{49}$$

where Λ = diag (λ) denotes a diagonal matrix whose diagonal elements are formed by λ and $e = [1,...,1]^T$. Here, F, G, and H are the Jacobian matrix of f(x), g(x), and h(x), respectively. From (44), since $s \geq 0$ and $\mu > 0$, then $\lambda \leq 0$. Using $r = R\pi$ and $s = -f(x)$ then (44)–(49) can be written as a system of nonlinear equations as

$$\begin{bmatrix} \Lambda f(x) = -\mu e \\ g(x) \\ R\pi - z + h(x) \\ F^T\lambda + G^T\rho + H^T\pi \end{bmatrix} = 0 \tag{50}$$

The problem of state estimation is to find λ, ρ, π, and x that satisfies (50) and all constraints in (42). The solution of the problem formulation of state estimation may be obtained by nonlinear constrained optimization solvers, e.g. Ipopt (Interior Point Optimizer) [71]. However, due to the state variables, i.e., transformer parameters, line temperatures and weather states, are included and the transmission line parameters, i.e. the series and the shunt admittance matrices, have to be re – evaluated when the line's conductor temperature is updated, this increases the computational burden to the solver. In this work, the method based on Mehrotra's predictor–corrector interior point [72] is applied to solve the constrained optimization problem.

Numerical Results

The proposed method has been implemented in MATLAB environment. All simulations are performed on a personal computer with an Intel Core i7 – 7700 CPU at 3.60 GHz and 16 GB of main memory. The standard deviations of the measurements are shown in Table 6. The Gaussian noise with zero mean are added to the corresponding true values obtained from the temperature – dependent three – phase optimal power flow algorithm [73] for measurement uncertainty simulation. The convergence tolerance is set to 10^{-4} for the bus voltage, line temperature, and transformer state variables. The convergence tolerance is set to 10^{-2} for the weather states using data scaling in the solving of the state estimation optimization problem.

Table 6 The standard deviations of the measurements

Measurement	Standard deviation
Voltage phasor	0.1 %
Current phasor	0.1 %
Phase angle	0.097 °
Voltage magnitude	1.0 %
Power	2.0 %
Temperature	0.17 °C
Wind speed	0.17 m/s
Wind direction	1.15 °
Solar radiation	3.16 W/m^2

Description of the three – phase test systems

The standard IEEE 30 – bus and 118 – bus systems have been modified and used as three – phase test networks. The line data of the standard IEEE 30 – bus and 118 – bus systems are considered as positive sequence parameters and the length of the overhead line is obtained based on the positive sequence reactance. The physical geometry, conductor data, and earth resistivity of the transmission line are used to compute the three – phase series and shunt parameters of each transmission line in both test networks. It is assumed that the average temperature of each phase conductor is equal. The average temperature of each earth wire conductor equals the estimated ambient temperature. The variation of sag at the mid – span dependent on the line temperature is considered. Three – phase representation of each transformer is done based on the available transformer parameters obtained from the standard systems. While transformer winding connections are assumed. Additionally, the weather data, untransposed transmission lines and three – phase unbalanced load conditions are simulated.

The Modified IEEE 30 – bus System

A single – line diagram of the modified IEEE 30 – bus system as show in Figure 24, operated at 132 – and 33 kV nominal voltage levels. The phase conductors of the 132 – and 33 kV overhead lines are chosen to be Panther and Leopard conductors, respectively. Two earth wires are employed for the 132 kV overhead line, while one earth wire is used for the 33 kV overhead line. The transformers connecting buses 4 – 12, 6 – 9, 6 – 10, and 28 – 27 are simulated as the three – phase wye – delta grounding transformers. They are the tap changing transformers where their tap and leakage admittance parameters are the estimated state variables. The three – phase grounded wye – wye interconnection transformers are used for the transformers connecting buses 9 – 10, 9 – 11, and 12 – 13. For the state estimation, the parameters of the wye – wye transformers in this test system are known. The simulation results obtained from the three – phase optimal power flow [72] determines that maximum temperature of conductor is 88°C for the modified IEEE 30 – bus system case.

The Modified IEEE 118 – bus System

The modified IEEE 118 – bus system operates at 345 – and 138 kV nominal voltage levels. It consists of 171 overhead lines and 9 transformers. The phase conductors of the 345 – and 138 kV overhead lines are chosen to be Goat and Panther conductors, respectively. Two earth wires are employed for all overhead lines. All three – phase transformers are tap changing transformers in which their configurations are grounded wye – delta winding connections. The tap and leakage admittance parameters are the estimated state variables for each three – phase transformer. The three – phase optimal power flow simulation results indicate that maximum temperature of conductor is 99°C for this test system.

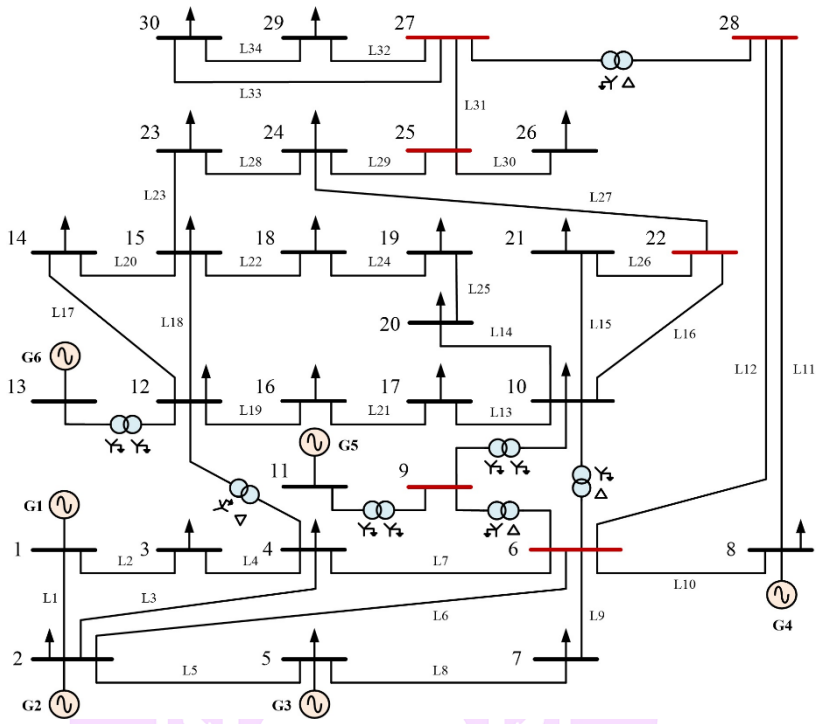

Figure 24 A single – line diagram of the modified IEEE 30 – bus system including transformer winding configuration.

Effects of Line Conductor's Temperature

To demonstrate the influence of line temperature on the state estimation considering transformer parameters as the estimated state variables, two cases have been conducted on the modified IEEE 30 – bus systems and 118 – bus systems as follows,

Case 1: Two tests using the conventional method have been performed and the obtained results are compared with the proposed method. In these tests, each line temperature is fixed at 20°C and 90°C, respectively, while the true values of measurements are employed for the state estimation in this case.

Case 2: Each line temperature is fixed at 90°C for the conventional method, and the obtained results are compared with the proposed method. The Gaussian noise are added to the measurement data and 100 Monte – Carlo simulations have been performed.

The types and the positions of the measurement systems of the both test systems are provided in Table 7. Those measurements give three – phase measured values for the two test cases.

Table 7 The types and the positions of the measurement systems

Measurement type	Measurement location	
	IEEE 30 – bus	IEEE 118 – bus
Voltage phasors	1, 4, 5, 6, 9, 11, 13, 15, 16, 19, 21, 25, 26, 27, 28, 29, 30	1, 4, 6, 8, 10, 11, 12, 15, 19, 23, 24, 25, 26, 27, 31, 33, 35, 40, 43, 46, 49, 54, 55, 57, 61, 64, 66, 69, 70, 72, 77, 80, 85, 87, 90, 92, 100, 102, 103, 105, 112, 114
Current phasors	1 – 2, 1 – 3, 4 – 2, 4 – 3, 4 – 6, 5 – 2, 5 – 7, 6 – 28, 15 – 12, 15 – 14, 15 – 18, 15 – 23, 16 – 17, 19 – 18, 19 – 20, 21 – 22, 25 – 24, 26 – 25, 28 – 6, 28 – 8, 29 – 27, 30 – 29,	1 – 2, 1 – 3, 4 – 5, 4 – 11, 6 – 5, 6 – 7, 8 – 9, 10 – 9, 11 – 5, 12 – 2, 12 – 7, 12 – 11, 12 – 14, 12 – 16, 12 – 117, 15 – 13, 15 – 14, 15 – 17, 19 – 15, 19 – 18, 19 – 20, 19 – 34, 23 – 22, 23 – 24, 23 – 25, 23 – 32, 24 – 70, 24 – 72, 25 – 23, 26 – 30, 27 – 25, 27 – 28, 27 – 115, 31 – 29, 31 – 32, 33 – 15, 33 – 37, 35 – 36, 35 – 37, 40 – 39, 40 – 41, 40 – 42, 43 – 44, 46 – 45, 46 – 47, 46 – 48, 49 – 42, 49 – 45, 49 – 47, 49 – 48, 49 – 51, 49 – 54, 49 – 66, 54 – 53, 54 – 55, 54 – 56, 54 – 59, 55 – 56, 55 – 59, 57 – 56, 61 – 59, 61 – 60, 61 – 62, 64 – 63, 64 – 65, 66 – 62, 66 – 67, 69 – 47, 69 – 49, 69 – 70, 69 – 75, 70 – 24, 70 – 71, 70 – 74, 70 – 75, 72 – 71, 73 – 71, 77 – 75, 77 – 76, 77 – 78, 77 – 82, 78 – 79, 80 – 96, 80 – 97, 80 – 98, 80 – 99, 85 – 83, 85 – 84, 85 – 86, 85 – 88,

Table 7 (cont.) The types and the positions of the measurement systems

Measurement type	Measurement location	
	IEEE 30 – bus	IEEE 118 – bus
Current phasors		87 – 86, 90 – 89, 92 – 91, 92 – 93, 92 – 94, 92 – 100, 92 – 102, 100 – 94, 100 – 98, 100 – 99, 100 – 101, 100 – 103, 100 – 104, 100 – 106, 102 – 101, 103 – 104, 103 – 110, 105 – 104, 105 – 106, 105 – 107, 105 – 108, 112 – 110, 114 – 32, 114 – 115
Voltage magnitude	7, 10, 12, 17, 18, 24	3, 5, 17, 21, 30, 33, 34, 37, 38, 39, 43, 45, 51, 56, 59, 60, 63, 65, 73, 74, 76, 83, 86, 94, 96, 106, 109, 110
Power flow measurement	7 – 6, 8 – 6, 10 – 17, 10 – 20, 10 – 21, 12 – 14, 12 – 16, 24 – 22, 24 – 23, 27 – 30, 4 – 12, 12 – 4, 6 – 9, 9 – 6, 6 – 10, 10 – 6, 9 – 10, 10 – 9, 9 – 11, 11 – 9, 12 – 13, 13 – 12, 27 – 28, 28 – 27	3 – 5, 3 – 12, 11 – 13, 17 – 16, 17 – 18, 17 – 31, 17 – 113, 21 – 20, 21 – 22, 23 – 24, 24 – 70, 24 – 72, 28 – 29, 32 – 113, 32 – 114, 33 – 15, 33 – 37, 34 – 36, 34 – 37, 34 – 43, 39 – 37, 45 – 44, 50 – 49, 50 – 57, 51 – 52, 52 – 53, 56 – 58, 56 – 59, 58 – 51, 59 – 60, 62 – 67, 65 – 38, 65 – 68, 68 – 81, 68 – 116, 71 – 72, 74 – 75, 76 – 118, 80 – 77, 82 – 83, 82 – 96, 83 – 84, 89 – 88, 94 – 93, 94 – 95, 96 – 94, 96 – 95, 96 – 97, 106 – 107, 109 – 108, 110 – 111, 5 – 8, 8 – 5, 25 – 26, 26 – 25, 17 – 30, 30 – 17, 38 – 37, 37 – 38, 59 – 63, 63 – 59, 61 – 64, 64 – 61, 66 – 65, 65 – 66,

Table 7 (cont.) The types and the positions of the measurement systems

Measurement type	Measurement location	
	IEEE 30 – bus	IEEE 118 – bus
		69 – 68, 68 – 69, 80 – 81, 81 – 80
Power injection measurement	10, 17, 24	39, 43, 101, 118

In case 1 of the modified IEEE 30 – bus system, the difference of bus voltage phasors (phase A, B and C) between the estimated state variables and their actual values is shown in Figures 25, 26, and 27, respectively. The results obtained through the proposed method, show the estimation errors of the bus voltage magnitudes and the phase angles close to zero. In contrast, the conventional method yields the estimation errors under the true measurement data. The errors of tap and leakage reactance of each transformer are shown in Figure 28. It can be seen that the estimation transformer parameters obtained by the conventional method is larger than of the proposed method. The results show very accurate estimation in both approaches.

In case 1 of the modified IEEE 118 – bus system, the difference of bus voltage phasors (phase A, B and C) between the estimated state variables and their actual values is shown in Figures 29, 30, and 31, respectively. While the errors of tap and leakage reactance of each transformer are shown in Figure 32. It can be seen that using the proposed method, the estimation errors close to zero similar to the case 1 of the modified IEEE 30 – bus system when there is no measurement noise.

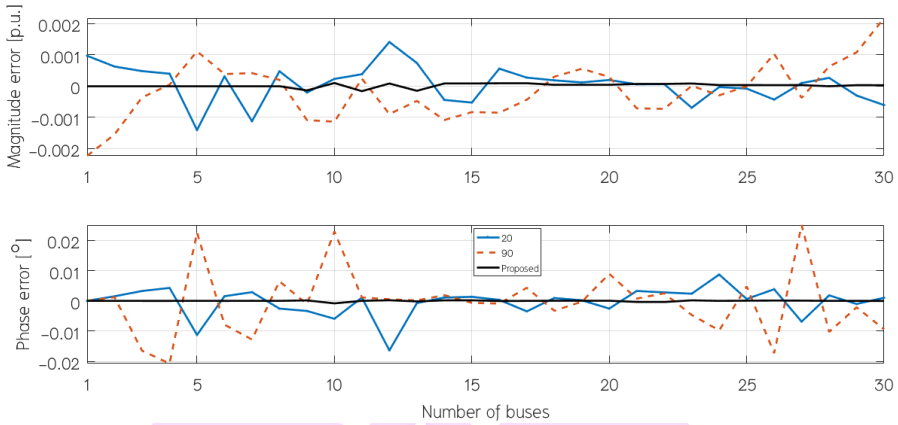

Figure 25 The voltage errors (phase A) for the 30 – bus network in case 1.

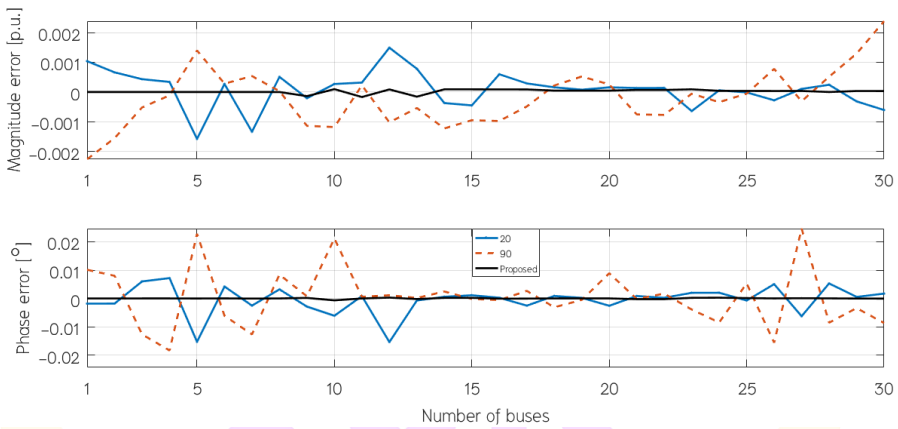

Figure 26 The voltage errors (phase B) for the 30 – bus network in case 1.

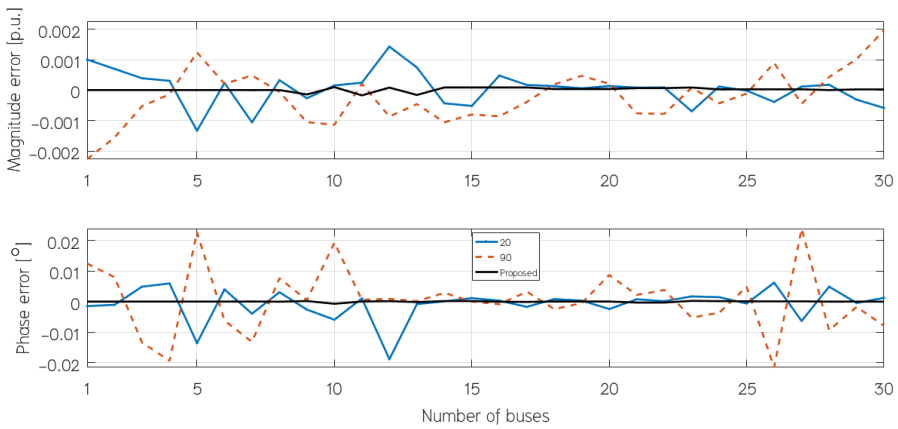

Figure 27 The voltage errors (phase C) for the 30 – bus network in case 1.

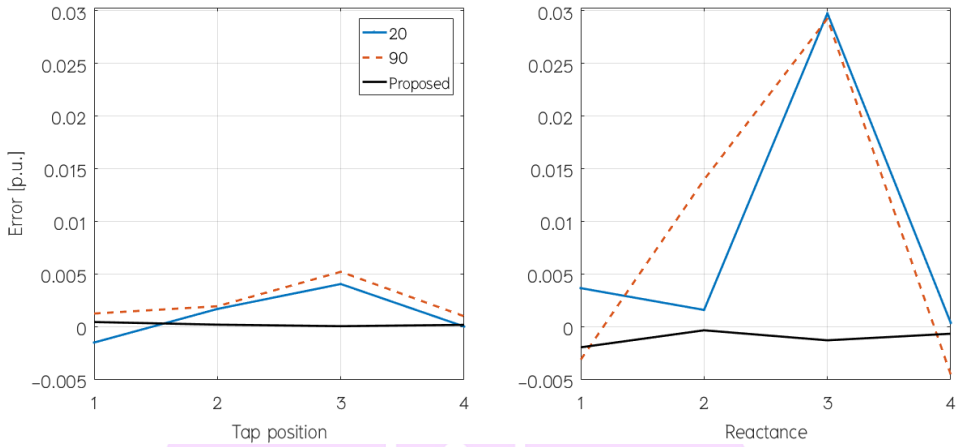

Figure 28 The transformer parameter errors for the 30 – bus system in case 1.

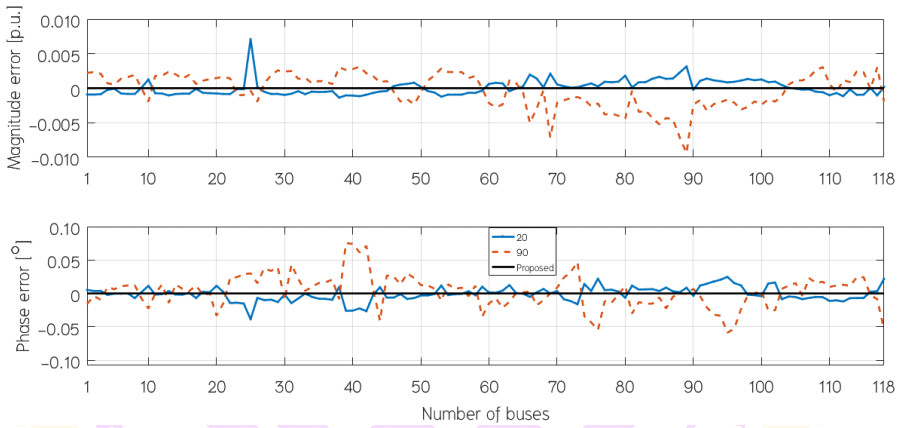

Figure 29 The voltage errors (phase A) for the 118 – bus network in case 1.

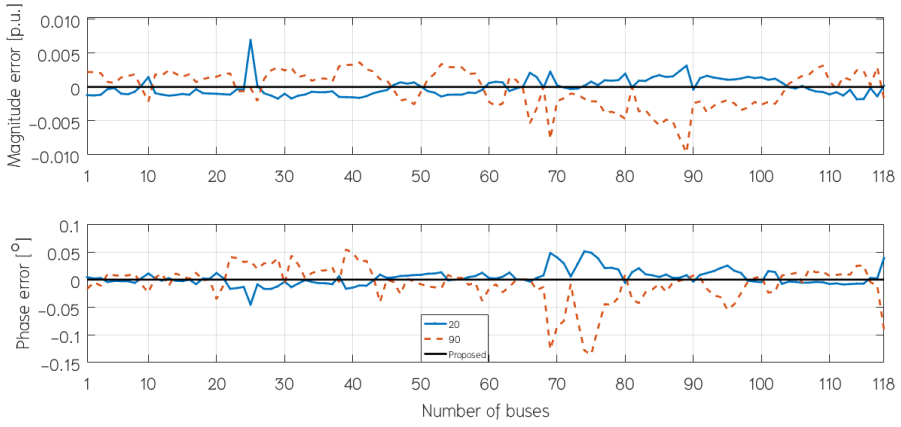

Figure 30 The voltage errors (phase B) for the 118 – bus network in case 1.

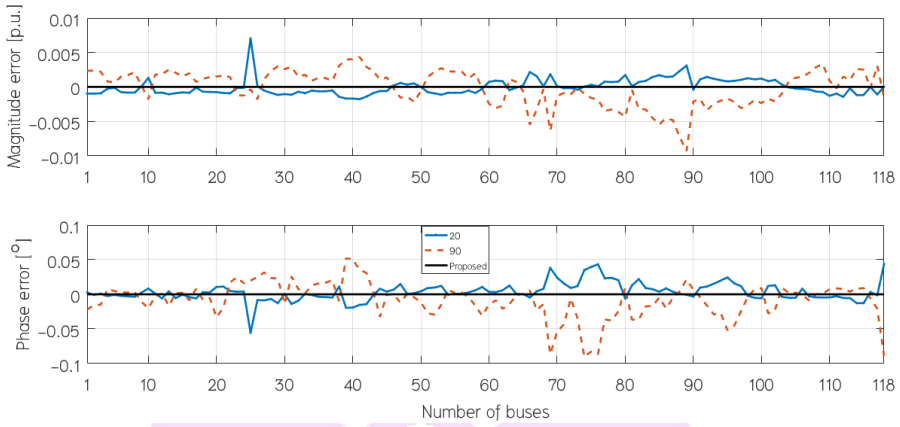

Figure 31 The voltage errors (phase C) for the 118 – bus network in case 1.

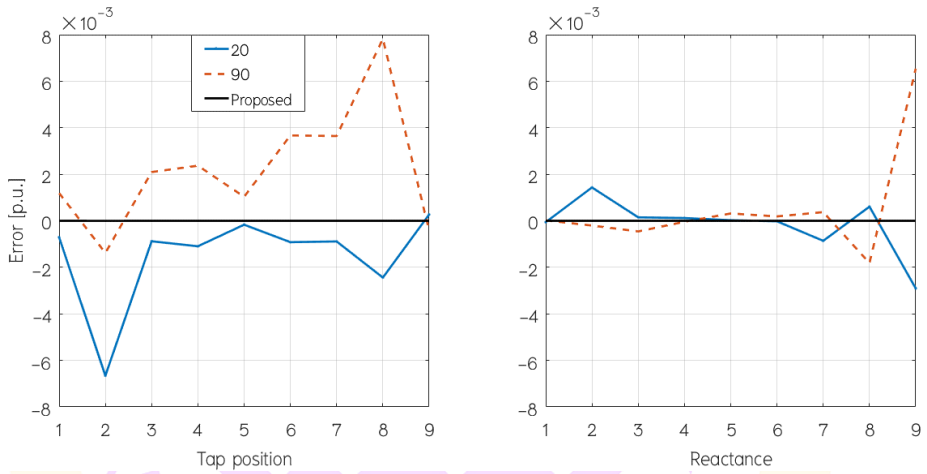

Figure 32 The transformer parameter errors for the 118 – bus system in case 1.

In case 2 of the modified IEEE 30 – bus system, an example of the difference of bus voltage phasors (phase A, B and C) between the estimated state variables and their actual values in one simulation is shown in Figures 33, 34, and 35, respectively. The errors of tap and leakage reactance of each transformer obtained from the simulation is shown in Figure 36. The parameters no. 1 to 4 in Figure 36, corresponding to the three – phase wye – delta grounding transformers connecting buses 4 – 12, 6 – 9, 6 – 10, and 28 – 27, respectively. The histograms of the objective function and the largest normalized residual, rn, max, are shown in Figure 37. It should be noted that the largest normalized residual test [74] is usually applied to WLS state estimation to detect bad data. These

results show that 9 percent of the estimations using the conventional method provides unreliable estimated states for the modified IEEE 30 – bus system since it is determined that bad measurement data is detected, i.e. rn, max > 4. In contrast, the proposed method can provide the reliable estimations for all Monte – Carlo simulations in this test case. The percentage error of the average temperature of line obtained from the proposed method is shown in Figure 38.

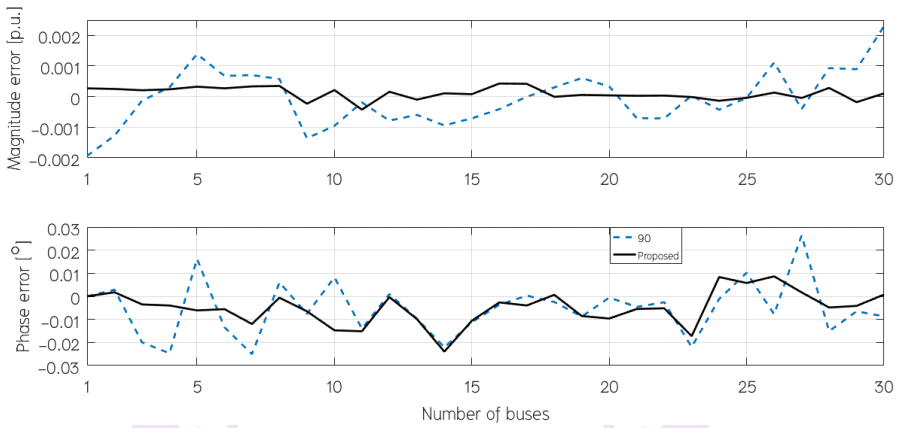

Figure 33 The voltage errors (phase A) for the 30 – bus network in case 2.

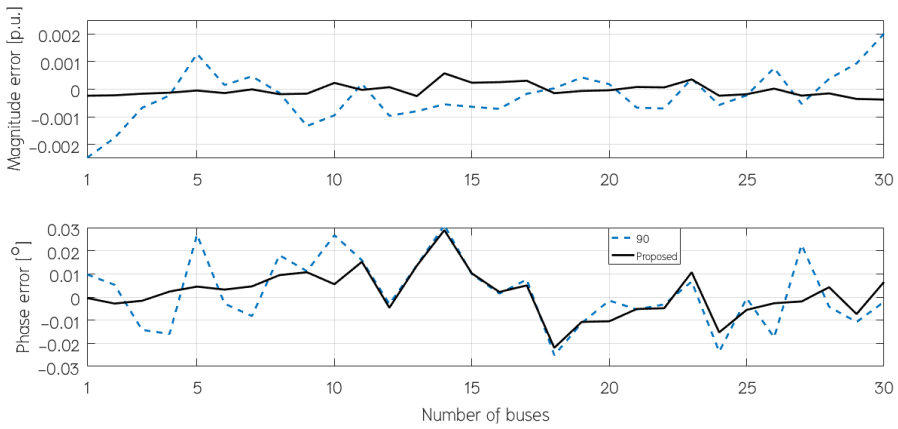

Figure 34 The voltage errors (phase B) for the 30 – bus network in case 2.

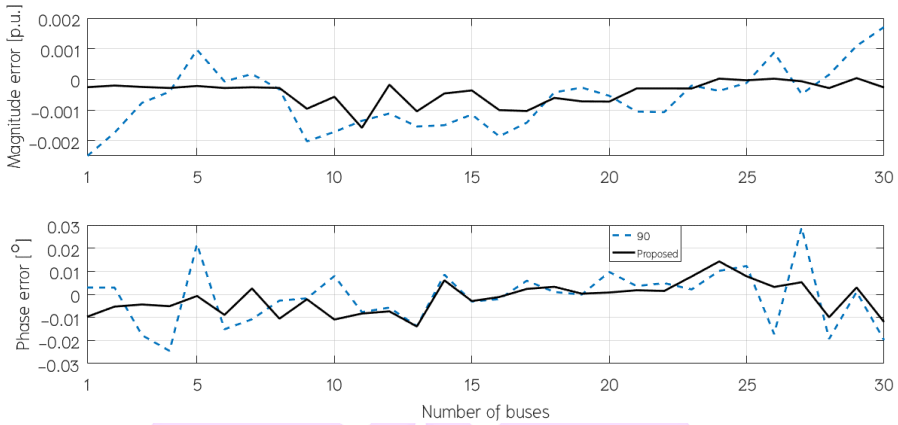

Figure 35 The voltage errors (phase C) for the 30 – bus network in case 2.

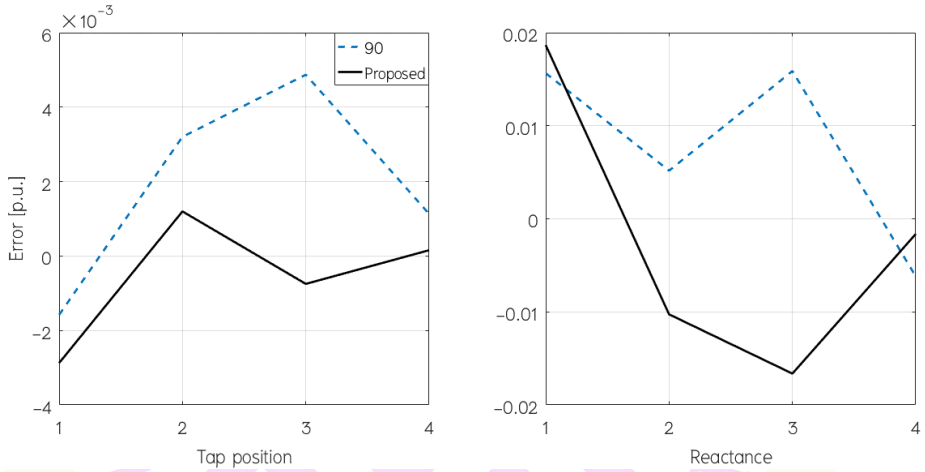

Figure 36 The transformer parameter errors for the 30 – bus system in case 2.

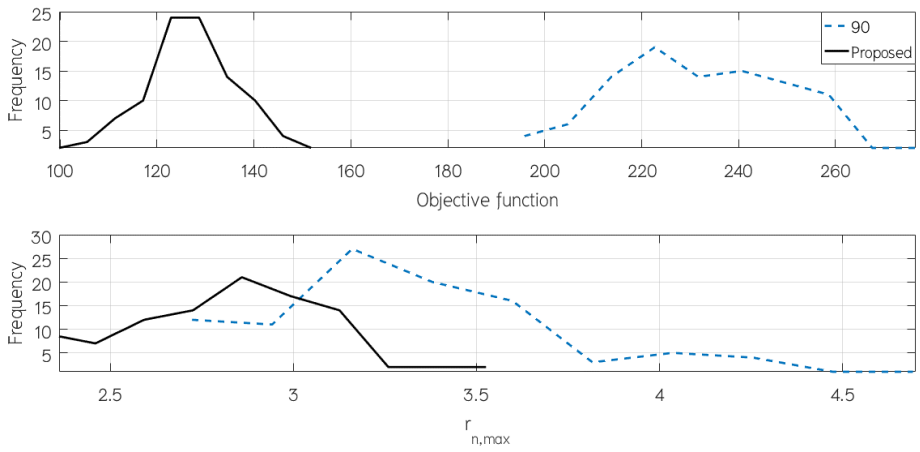

Figure 37 Histograms of ϕ and $r_{n,max}$ for the 30 – bus system in case 2.

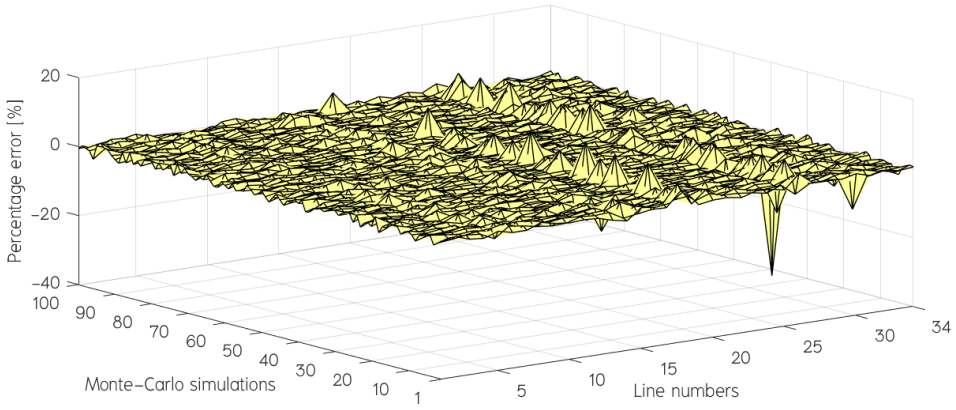

Figure 38 The errors of line temperatures for the 30 – bus system in case 2.

In case 2 of the modified IEEE 118 – bus system, the difference of bus voltage phasors (phase A, B and C) between the estimated state variables and their actual values in one simulation is shown in Figures 39, 40, and 41, respectively. The errors of tap and leakage reactance of each transformer is shown in Figure 41. The parameters no. 1 to 9 in Figure 42, corresponding to the three – phase wye – delta grounding transformers connecting buses 8 – 5, 26 – 25, 30 – 17, 38 – 37, 63 – 59, 64 – 61, 65 – 66, 68 – 69, and 81 – 80, respectively. Additionally, the histograms of the objective function and the largest normalized residual, rn, max, are shown in Figure 43. It can be seen that the conventional method gives unreliable estimated states for the modified 118 – bus system since its solution is detected as bad data occurs in all simulations, while only 1 percent of the estimations obtained by the proposed method is unreliable.

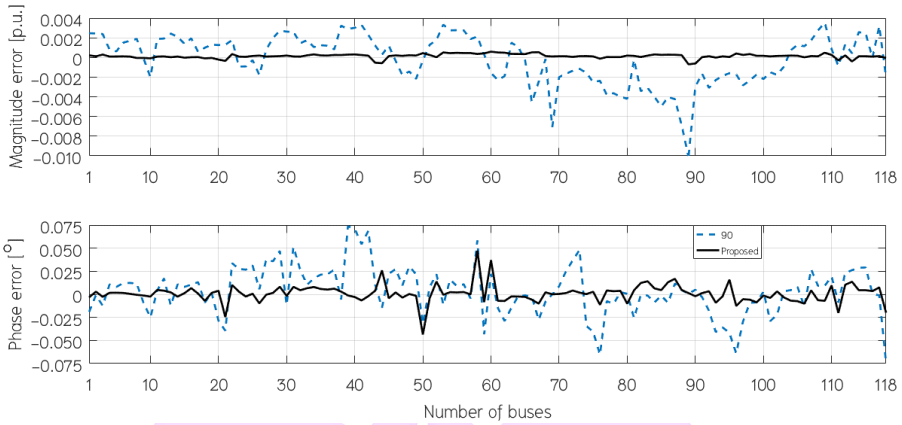

Figure 39 The voltage errors (phase A) for the 118 – bus network in case 2.

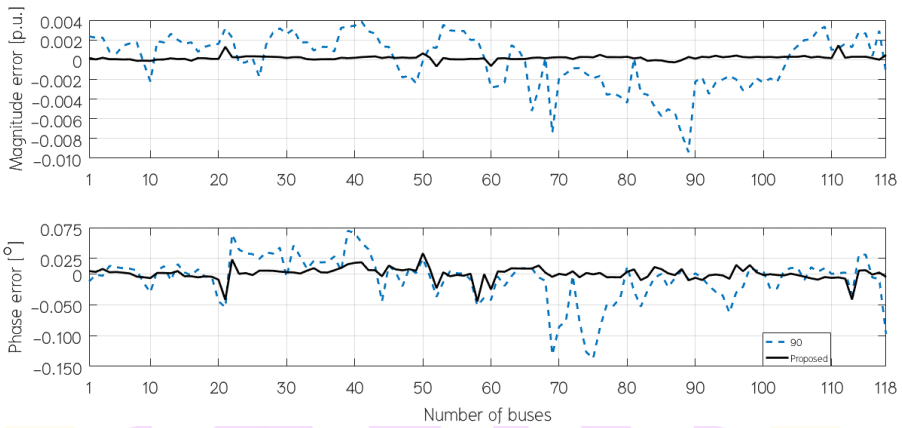

Figure 40 The voltage errors (phase B) for the 118 – bus network in case 2.

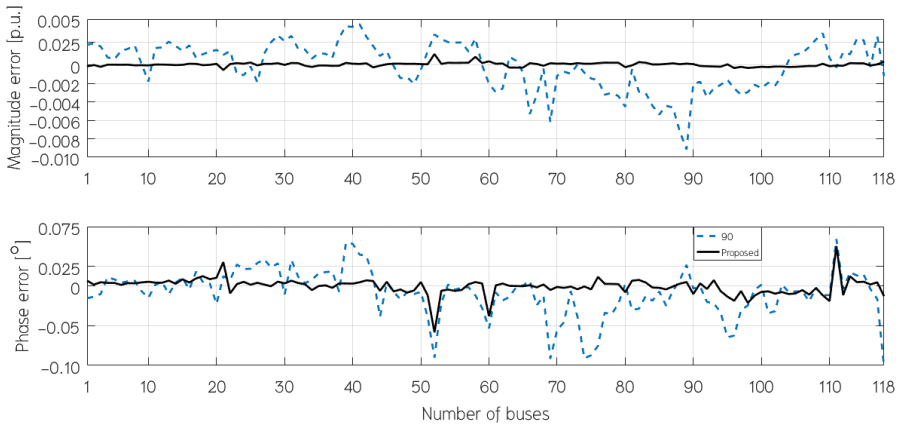

Figure 41 The voltage errors (phase C) for the 118 – bus network in case 2.

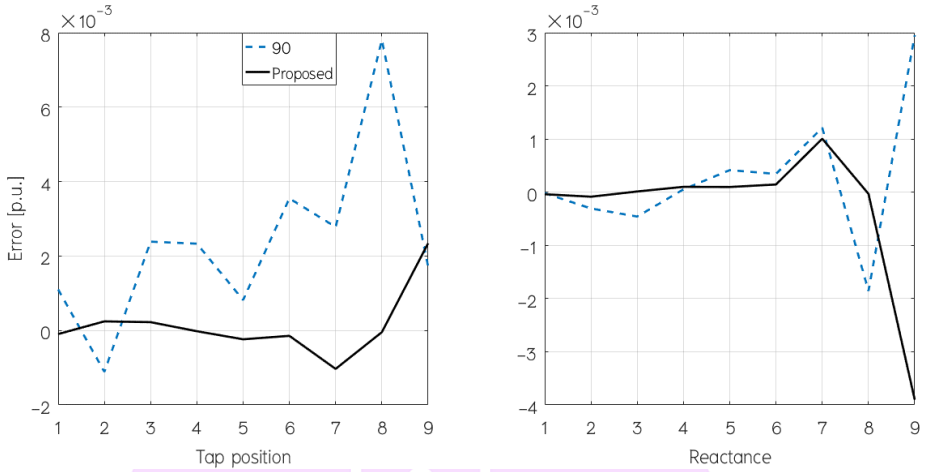

Figure 42 The transformer parameter errors for the 118 – bus system in case 2.

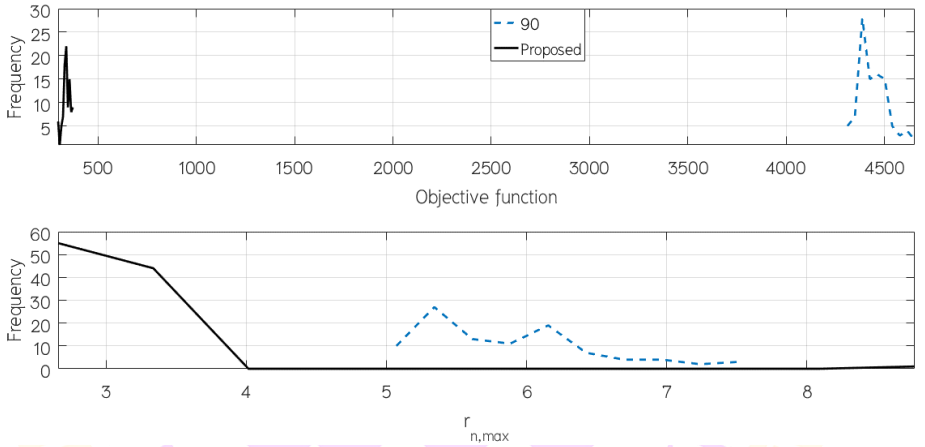

Figure 43 Histograms of ϕ and $r_{n,max}$ for the 118 – bus system in case 2.

Table 8 The average computation time in seconds

Test system	Conventional method	Proposed method
IEEE 30 – bus	3.74	10.53
IEEE 118 – bus	12.36	32.17

The average computation time required for the conventional and the proposed methods in case 2 is summarized in Table 8. It can be seen that the proposed method requires larger computation time because including the weather base model of the transmission line into the proposed state estimation yields a complexity optimization problem. The accurate estimated states are typically important than the computation effort as the computation time can be enhanced by high performance computer and efficient programming.

Estimation of The Top – Oil and The Hot – Spot Winding Temperatures of Transformer

The estimated states obtained from the proposed method in case 2 of the modified IEEE 30 – bus system are used to evaluate the top – oil and the hot – spot winding temperatures of the power transformers connecting buses 4 – 12, 6 – 9, 6 – 10, and 28 – 27. The estimated ambient temperatures which correspond to the transmission lines 3 – 4, 10 – 17, 10 – 17, and 25 – 27, and the estimated three – phase power on the primary sides of those transformers are employed. The rated power of each transformer is 25 MVA and its essential data is given in Table 4 of Chapter 3. It is assumed that the variation of the data due to changing of the tap and the reactance values of the transformer is ignored. The time step of each state estimation is assumed to be 30 seconds. Therefore, the interval time is 50 minutes obtained from the 100 Monte – Carlo simulations. The estimated thermal states, which are the top – oil and the hot – spot winding temperatures, of the three – phase wye – delta grounding transformers connecting buses 4 – 12, 6 – 9, 6 – 10, and 28 – 27, are shown in Figures 44, 45, 46, and 47, respectively. True values of the top – oil and the hot – spot winding temperature are calculated from equation (35), and (36) using the true values of power and ambient temperature. It can be observed that the estimated temperatures are close to the true values.

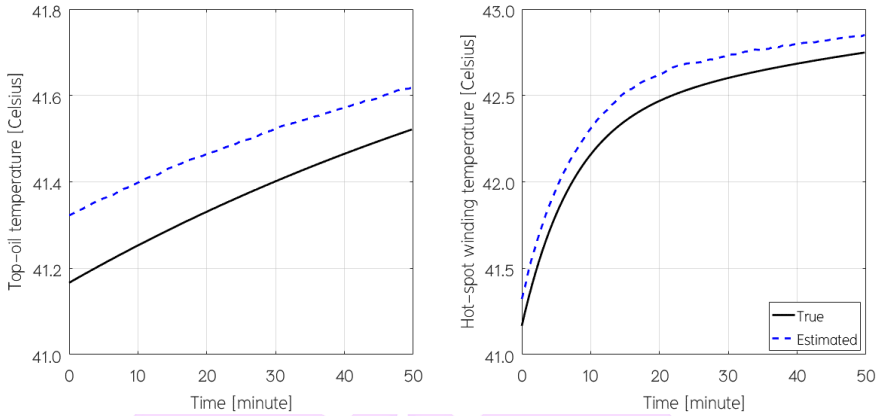

Figure 44 The thermal states of transformer connecting buses 4 – 12.

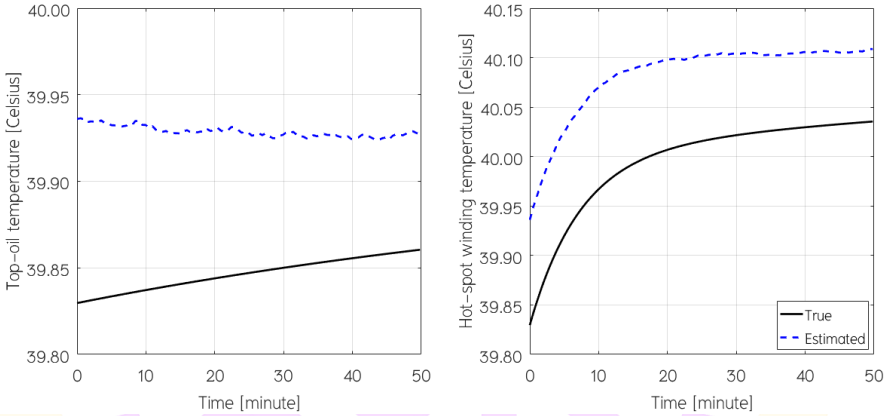

Figure 45 The thermal states of transformer connecting buses 6 – 9.

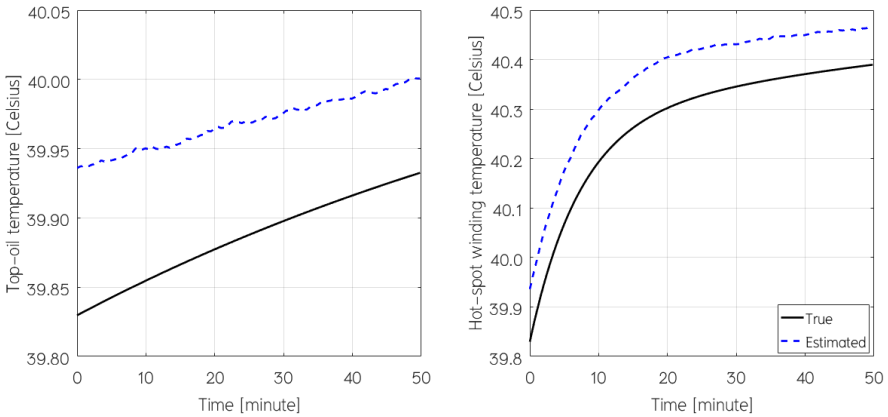

Figure 46 The thermal states of transformer connecting buses 6 – 10.

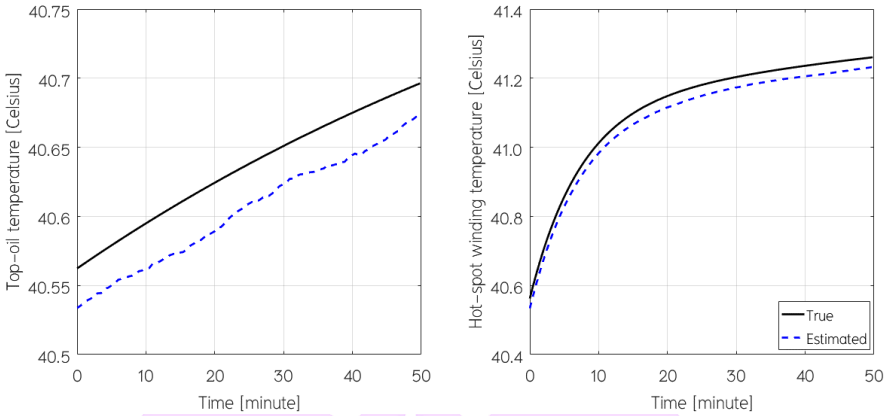

Figure 47 The thermal states of transformer connecting buses 28 – 27.

In case 2 of the modified IEEE 118 – bus system, it is assumed that the rated power of the power transformers connecting buses 65 – 66 and 81 – 80 is chosen to be 25 MVA while the rated power of other power transformers is 250 MVA. In addition, the estimated ambient temperatures of some transmission lines linked with the transformers are used. The top – oil and the hot – spot winding temperatures of all power transformers are estimated using the proposed method and the results are shown in Figures 48, 49, 50, 51, 52, 53, 54, 55, and 56. It can be observed that the estimated temperatures are close to the true values similarly to the modified IEEE 30 – bus test case.

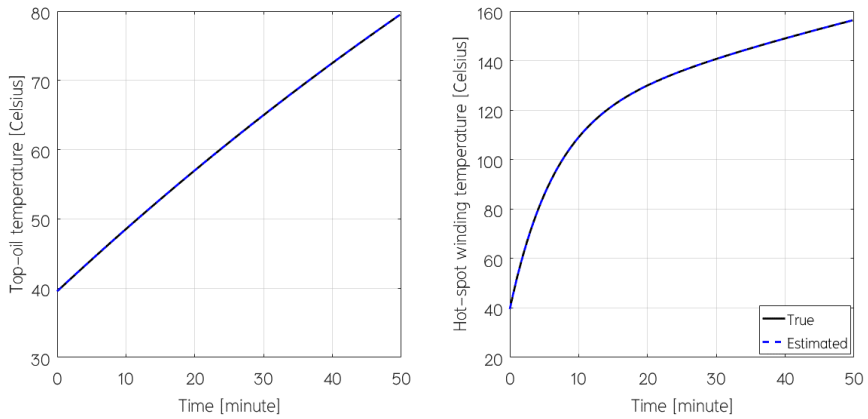

Figure 48 The thermal states of transformer connecting buses 8 – 5.

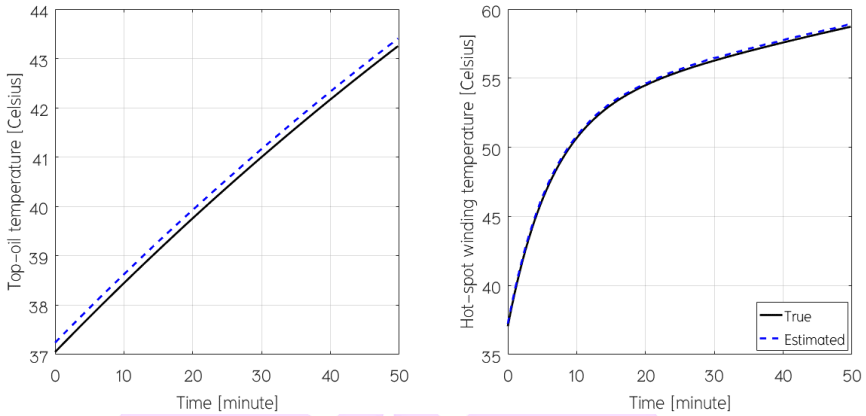

Figure 49 The thermal states of transformer connecting buses 26 – 25.

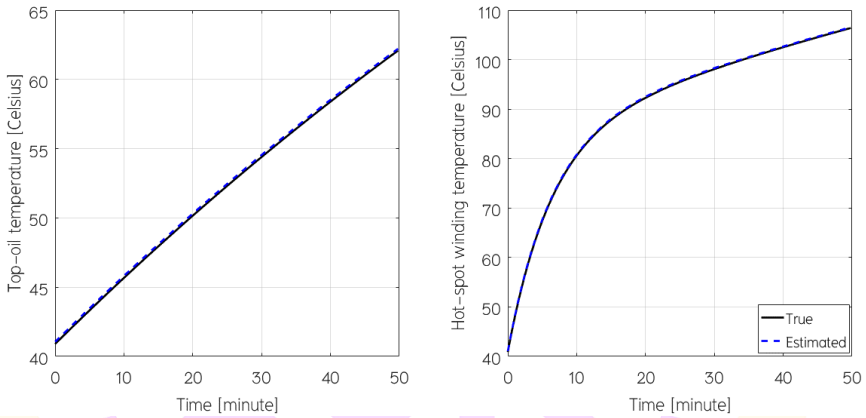

Figure 50 The thermal states of transformer connecting buses 30 – 17.

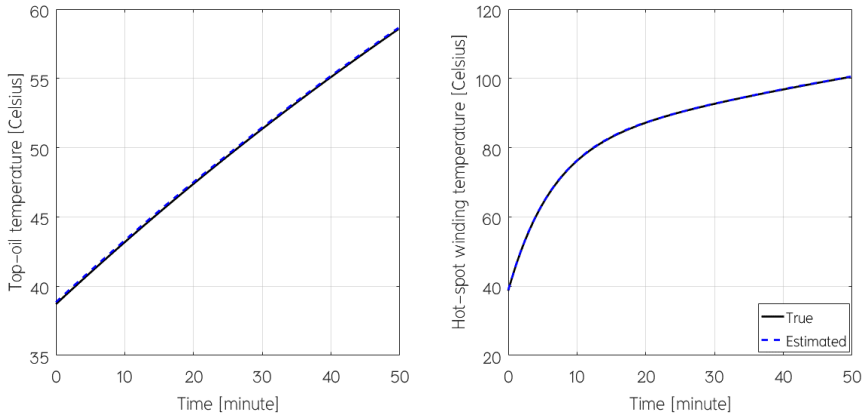

Figure 51 The thermal states of transformer connecting buses 38 – 37.

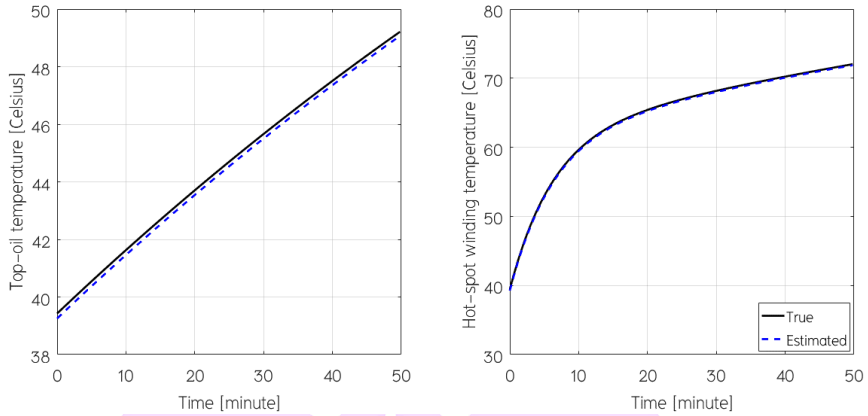

Figure 52 The thermal states of transformer connecting buses 63 – 59.

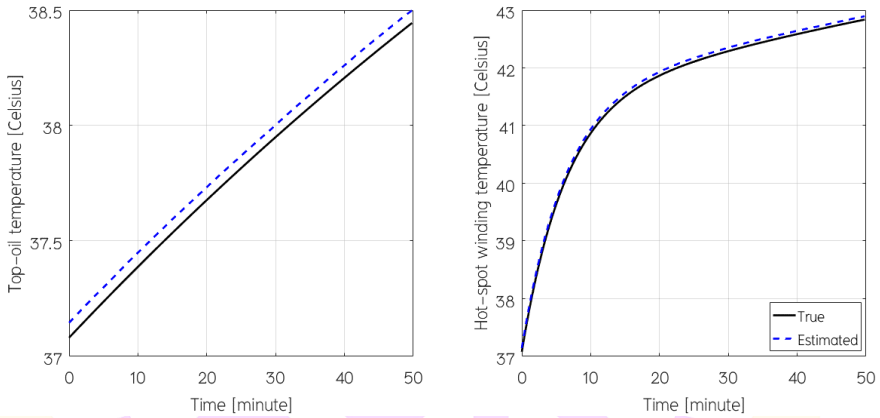

Figure 53 The thermal states of transformer connecting buses 64 – 61.

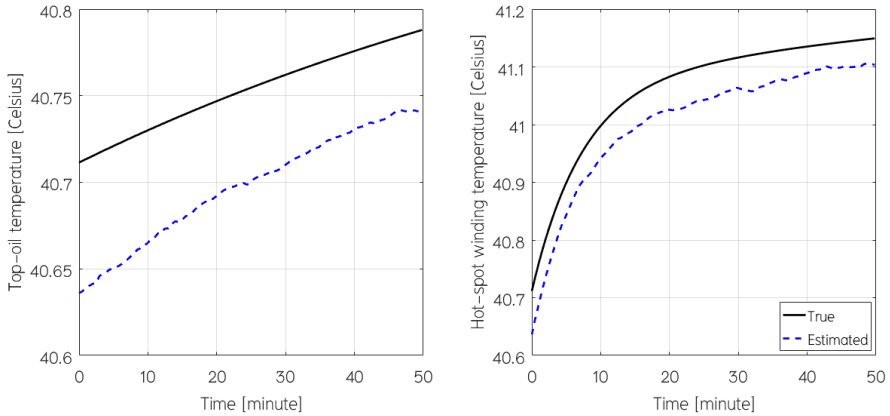

Figure 54 The thermal states of transformer connecting buses 65 – 66.

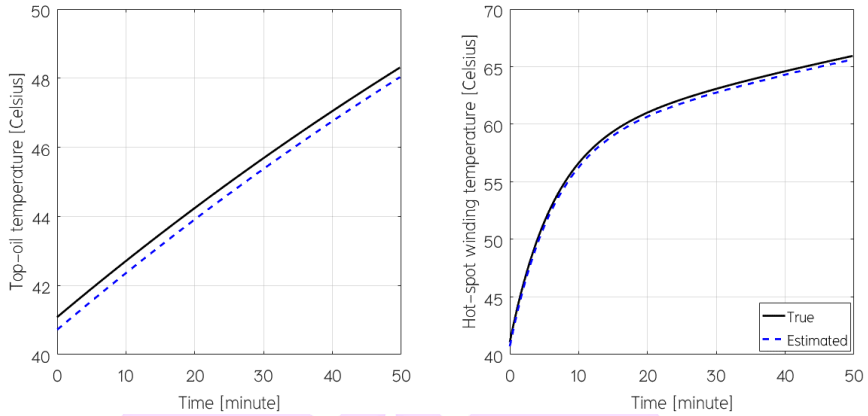

Figure 55 The thermal states of transformer connecting buses 68 – 69.

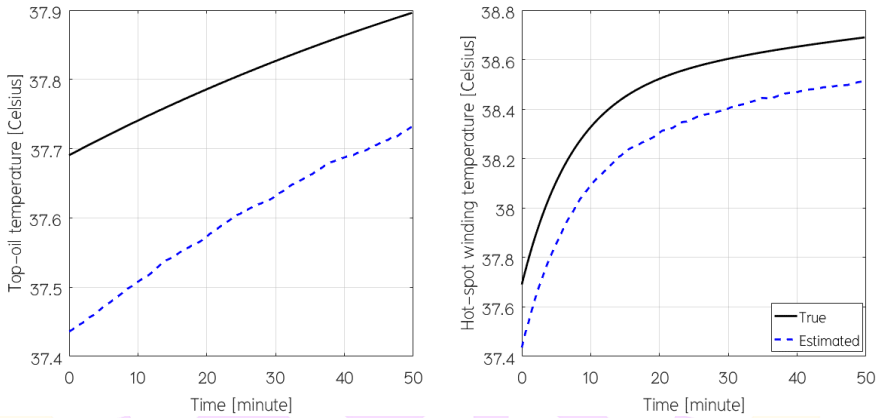

Figure 56 The thermal states of transformer connecting buses 81 – 80.

Conclusion

The state estimation strategy for estimating the thermal states of the transmission lines and the power in the three – phase power networks has been proposed. Firstly, the temperature – dependent state estimation of which the conductor temperatures of the transmission lines, the weather environment, and the transformer parameters are also considered as the estimated states, is performed. Then, the estimated states are used to estimate the transformer's thermal states, which are the top – oil and the hot – spot winding temperatures. The proposed state estimation method uses a set of measurements obtained from RTUs and PMUs devices without the tap position and the line temperature

measurements. The formulation of the state estimation as a constrained nonlinear optimization problem has been described. Two three – phase test systems have been used to demonstrate, and the results obtained from the proposed method has been compared with the conventional method in which all line temperatures are fixed. Comparison results show that the proposed method can improve the accuracy of the estimated state variables and successfully provides the estimated thermal states of both the transmission line and the transformer.

Chapter V

Conclusions and Further Research

Conclusions

Two algorithms have been proposed in this dissertation. First, an algorithm can be used to assess the voltage stability in the power systems when the thermal limit of the transmission line is also considered. The line voltage stability and the line ampacity indices which can be estimated using the same conventional measurements have been proposed. Their values should be less than unity in order to maintain the voltage stability and the line security of the buses and the line corresponding to the indices. By considering both line voltage stability and line ampacity indices, power systems could mitigate the risks of voltage collapse and excessive current in transmission line. The second algorithm is a temperature – dependent state estimation for three – phase power systems. The conductor temperatures of transmission lines, the transformer parameters, and the weather parameters are included as the estimated state variables. The estimation of top – oil and the hot – spot winding temperatures can be done using the proposed state estimation algorithm. Comparison results indicate that the proposed method outperforms the conventional method, which does not consider the transmission line temperature – dependency, in terms of accuracy and bad data detection.

Recommendations of Further Research

Although the state estimation method of power systems including the thermal states of the transmission line and the power transformer have been presented in this dissertation, the work may be further developed in some subjects as the follows.

- The thermal states of the power transformer may be added to the estimated state variables of the constrained state estimation problem.
- The practical transformer data for each tap position should be used.
- The underground cable temperature.

– Effect of harmonics propagation on the thermal modelling of the power system components.

– Bad data identification.

BIBLIOGRAPHY

BIBLIOGRAPHY

[1] J. P. Anthony, "Power transmission and distribution," In *Power Transmission and Distribution*: River Publishers, 2005, pp. 1 – 14.

[2] C. Barrows *et al.*, "The IEEE reliability test system: A proposed 2019 update," *IEEE Transactions on Power Systems,* vol. 35, no. 1, pp. 119 – 127, 2020, doi: 10.1109/TPWRS.2019.2925557.

[3] D. Cao *et al.*, "Reinforcement learning and its applications in modern power and energy systems: A Review," *Journal of Modern Power Systems and Clean Energy,* vol. 8, no. 6, pp. 1029 – 1042, 2020, doi: 10.35833/MPCE.2020.000552.

[4] Y. Chen, C. Wu, and J. Qi, "Data – driven power flow method based on exact linear regression equations," *Journal of Modern Power Systems and Clean Energy,* vol. 10, no. 3, pp. 800 – 804, 2022, doi: 10.35833/MPCE.2020.000738.

[5] S. Peyghami, P. Palensky, and F. Blaabjerg, "An overview on the reliability of modern power electronic based power systems," *IEEE Open Journal of Power Electronics,* vol. 1, pp. 34 – 50, 2020, doi: 10.1109/OJPEL.2020.2973926.

[6] A. S. Dobakhshari, M. Abdolmaleki, V. Terzija, and S. Azizi, "Online non – iterative estimation of transmission line and transformer parameters by SCADA data," *IEEE Transactions on Power Systems,* vol. 36, no. 3, pp. 2632 – 2641, 2021, doi: 10.1109/TPWRS.2020.3037997.

[7] S. Acharya and P. C. Tapre, "Life assessment of transformer using thermal models," in *2017 International Conference on Energy, Communication, Data Analytics and Soft Computing (ICECDS)*, 1 – 2 Aug. 2017 2017, pp. 3515 – 3520, doi: 10.1109/ICECDS.2017.8390114.

[8] Q. Xu, H. Zhang, Y. Cao, H. Qin, and Z. Gao, "Power system state estimation approach considering transmission line temperature," *Applied Sciences,* vol. 12, p. 10171, 10/10 2022, doi: 10.3390/app121910171.

[9] Y. – S. Cho and Y. Choi, "Methodology for Implementing the state estimation in renewable energy management systems," *Energies,* vol. 14, p. 2301, 04/19 2021, doi: 10.3390/en14082301.

[10] F. Fan, B. Stephen, K. Bell, D. Infield, and S. McArthur, "Impacts of measurement errors on real – time thermal rating estimation for overhead lines," *IEEE Transactions on Power Delivery,* vol. 38, no. 2, pp. 1086 – 1096, 2023, doi: 10.1109/TPWRD.2022.3205248.

[11] M. Bockarjova and G. Andersson, "Transmission line conductor temperature impact on state estimation accuracy," in *2007 IEEE Lausanne Power Tech*, 1 – 5 July 2007 2007, pp. 701 – 706, doi: 10.1109/PCT.2007.4538401.

[12] F. Wang, X. Zhou, P. Gao, and X. Xi, "Improved thermal circuit model of hot spot temperature in oil – immersed transformers based on heat distribution of winding," *Gaodianya Jishu/High Voltage Engineering,* vol. 41, pp. 895 – 901, 03/28 2015, doi: 10.13336/j.1003 – 6520.hve.2015.03.026.

[13] K. M. Takami, H. Gholnejad, and J. Mahmoudi, "Thermal and hot spot evaluations on oil immersed power Transformers by FEMLAB and MATLAB software's," in *2007 International Conference on Thermal, Mechanical and Multi – Physics Simulation Experiments in Microelectronics and Micro – Systems. EuroSime 2007*, 16 – 18 April 2007 2007, pp. 1 – 6, doi: 10.1109/ESIME.2007.359924.

[14] S. Almohaimeed and S. Suryanarayanan, *Steady – state analysis of the impact of temperature variations on a distribution transformer*. 2017, pp. 1 – 5.

[15] C. Rakpenthai and S. Uatrongjit, "Power system state and transmission line conductor temperature estimation," *IEEE Transactions on Power Systems,* vol. 32, no. 3, pp. 1818 – 1827, 2017, doi: 10.1109/TPWRS.2016.2601072.

[16] O. E. Gouda, G. M. Amer, and W. A. A. Salem, "Predicting transformer temperature rise and loss of life in the presence of harmonic load currents," *Ain Shams Engineering Journal,* vol. 3, no. 2, pp. 113 – 121, 2012/06/01/ 2012, doi: https://doi.org/10.1016/j.asej.2012.01.003.

[17] T. Cutsem and C. Vournas, "Voltage stability of electric power systems, 1998.

[18] "Estimating maximum loadability for weak bus identification using FVSI," *IEEE Power Engineering Review,* vol. 22, no. 11, pp. 50 – 52, 2002, doi: 10.1109/MPER.2002.4311799.

[19] V. Balamourougan, T. S. Sidhu, and M. S. Sachdev, "Technique for online prediction of voltage collapse," 2004.

[20] P. Kessel and H. Glavitsch, "Estimating the voltage stability of a power system," *IEEE Transactions on Power Delivery,* vol. 1, no. 3, pp. 346 – 354, 1986, doi: 10.1109/TPWRD.1986.4308013.

[21] I. Musirin and T. K. A. Rahman, "Novel fast voltage stability index (FVSI) for voltage stability analysis in power transmission system," in *Student Conference on Research and Development*, 17 – 17 July 2002 2002, pp. 265 – 268, doi: 10.1109/SCORED.2002.1033108.

[22] R. Tiwari, K. R. Niazi, and V. Gupta, "Line collapse proximity index for prediction of voltage collapse in power systems," *International Journal of Electrical Power & Energy Systems,* vol. 41, no. 1, pp. 105 – 111, 2012/10/01/ 2012, doi: https://doi.org/10.1016/j.ijepes.2012.03.022.

[23] A. Yazdanpanah – Goharrizi and R. Asghari, "A novel line stability index (NLSI) for voltage stability assessment of power systems," 2007.

[24] B. Ismail *et al.*, "New line voltage stability index (BVSI) for voltage stability assessment in power system: The Comparative Studies," *IEEE Access,* vol. 10, pp. 103906 – 103931, 2022, doi: 10.1109/ACCESS.2022.3204792.

[25] S. Mokred, Y. Wang, and T. Chen, "Modern voltage stability index for prediction of voltage collapse and estimation of maximum load – ability for weak buses and critical lines identification," *International Journal of Electrical Power & Energy Systems,* vol. 145, p. 108596, 2023/02/01/ 2023, doi: https://doi.org/10.1016/j.ijepes.2022.108596.

[26] S. Ratra, R. Tiwari, and K. R. Niazi, "Voltage stability assessment in power systems using line voltage stability index," *Computers & Electrical Engineering,* vol. 70, pp. 199 – 211, 2018/08/01/ 2018, doi: https://doi.org/10.1016/j.compeleceng.2017.12.046.

[27] P. A. Lof, T. Smed, G. Andersson, and D. J. Hill, "Fast calculation of a voltage stability index," *IEEE Transactions on Power Systems,* vol. 7, no. 1, pp. 54 – 64, 1992, doi: 10.1109/59.141687.

[28] A. Berizzi, P. Finazzi, D. Dosi, P. Marannino, and S. Corsi, "First and second order methods for voltage collapse assessment and security enhancement," *IEEE Transactions on Power Systems,* vol. 13, no. 2, pp. 543 – 551, 1998, doi: 10.1109/59.667380.

[29] B. Gao, G. K. Morison, and P. Kundur, "Voltage stability evaluation using modal analysis," *IEEE Transactions on Power Systems,* vol. 7, no. 4, pp. 1529 – 1542, 1992, doi: 10.1109/59.207377.

[30] A. C. Z. d. Souza, C. A. Canizares, and V. H. Quintana, "New techniques to speed up voltage collapse computations using tangent vectors," *IEEE Transactions on Power Systems,* vol. 12, no. 3, pp. 1380 – 1387, 1997, doi: 10.1109/59.630485.

[31] C. A. Canizares, A. C. Z. D. Souza, and V. H. Quintana, "Comparison of performance indices for detection of proximity to voltage collapse," *IEEE Transactions on Power Systems,* vol. 11, no. 3, pp. 1441 – 1450, 1996, doi: 10.1109/59.535685.

[32] S. Corsi and G. N. Taranto, "A real – time voltage instability identification algorithm based on local phasor measurements," *IEEE Transactions on Power Systems,* vol. 23, no. 3, pp. 1271 – 1279, 2008, doi: 10.1109/TPWRS.2008.922586.

[33] K. P. Guddanti, A. R. R. Matavalam, and Y. Weng, "PMU – based distributed non – Iterative algorithm for real – time voltage stability monitoring," *IEEE Transactions on Smart Grid,* vol. 11, no. 6, pp. 5203 – 5215, 2020, doi: 10.1109/TSG.2020.3007063.

[34] F. Hu, K. Sun, A. D. Rosso, E. Farantatos, and N. Bhatt, "Measurement – based real – time voltage stability monitoring for load areas," *IEEE Transactions on Power Systems,* vol. 31, no. 4, pp. 2787 – 2798, 2016, doi: 10.1109/TPWRS.2015.2477080.

[35] B. Milosevic and M. Begovic, "Voltage – stability protection and control using a wide – area network of phasor measurements," *IEEE Transactions on Power Systems,* vol. 18, no. 1, pp. 121 – 127, 2003, doi: 10.1109/TPWRS.2002.805018.

[36] I. Smon, G. Verbic, and F. Gubina, "Local voltage – stability index using tellegen's theorem," *IEEE Transactions on Power Systems,* vol. 21, no. 3, pp. 1267 – 1275, 2006, doi: 10.1109/TPWRS.2006.876702.

[37] K. Vu, M. M. Begovic, D. Novosel, and M. M. Saha, "Use of local measurements to estimate voltage – stability margin," *IEEE Transactions on Power Systems,* vol. 14, no. 3, pp. 1029 – 1035, 1999, doi: 10.1109/59.780916.

[38] H. Yuan, F. Li, H. Cui, X. Lu, D. Shi, and Z. Wang, "A measurement – based VSI for voltage dependent loads using angle difference between tangent lines of load and PV curves," *Electric Power Systems Research,* vol. 160, pp. 13 – 16, 2018/07/01/ 2018, doi: https://doi.org/10.1016/j.epsr.2018.01.021.

[39] A. R. R. Matavalam, S. M. H. Rizvi, A. K. Srivastava, and V. Ajjarapu, "Critical comparative analysis of measurement based centralized online voltage stability Indices," *IEEE Transactions on Power Systems,* vol. 37, no. 6, pp. 4618 – 4629, 2022, doi: 10.1109/TPWRS.2022.3145466.

[40] "IEEE standard for calculating the current – temperature relationship of bare overhead conductors," *IEEE Std 738 – 2012 (Revision of IEEE Std 738 – 2006 – Incorporates IEEE Std 738 – 2012 Cor 1 – 2013),* pp. 1 – 72, 2013, doi: 10.1109/IEEESTD.2013.6692858.

[41] D. A. Douglass, "Weather – dependent versus static thermal line ratings (power overhead lines)," *IEEE Transactions on Power Delivery,* vol. 3, no. 2, pp. 742 – 753, 1988, doi: 10.1109/61.4313.

[42] D. A. Douglass *et al.*, "A review of dynamic thermal line rating methods with forecasting," *IEEE Transactions on Power Delivery,* vol. 34, no. 6, pp. 2100 – 2109, 2019, doi: 10.1109/TPWRD.2019.2932054.

[43] R. Zimmerman, C. Murillo – Sanchez, and R. Thomas, "MATPOWER: Steady – state operations, planning, and analysis tools for power systems research and education," *IEEE Transactions on Power Systems,* vol. 26, pp. 12 – 19, 02/01 2011, doi: 10.1109/TPWRS.2010.2051168.

[44] X. Zhang, H. Yang, G. Zhou, Y. Zhao, and D. Guo, "Steady – state voltage stability assessment of new energy power systems with multi – quadrant power modes,"

Energy Reports, vol. 9, pp. 3851 – 3860, 2023/12/01/ 2023, doi: https://doi.org/10.1016/j.egyr.2023.02.093.

[45] M. Wydra and P. Kacejko, "Power system state estimation accuracy enhancement using temperature measurements of overhead line conductors," *Metrology and Measurement Systems,* vol. 23, 06/01 2016, doi: 10.1515/mms – 2016 – 0014.

[46] S. A. Almohaimeed and S. Suryanarayanan, "Steady – state analysis of the impact of temperature variations on a distribution transformer," in *2017 North American Power Symposium (NAPS)*, 17 – 19 Sept. 2017 2017, pp. 1 – 5, doi: 10.1109/NAPS.2017.8107174.

[47] M. Ariannik, A. A. Razi – Kazemi, and M. Lehtonen, "An approach on lifetime estimation of distribution transformers based on degree of polymerization," *Reliability Engineering & System Safety,* vol. 198, p. 106881, 2020/06/01/ 2020, doi: https://doi.org/10.1016/j.ress.2020.106881.

[48] M. T. Askari, M. Z. A. A. Kadir, W. F. W. Ahmad, and M. Izadi, "Investigate the effect of variations of ambient temperature on HST of transformer," in *2009 IEEE Student Conference on Research and Development (SCOReD)*, 16 – 18 Nov. 2009 2009, pp. 363 – 367, doi: 10.1109/SCORED.2009.5442998.

[49] S. Cho, "Parameter estimation for transformer modeling," 01/01 2002.

[50] A. Keyhani, S. M. Miri, and S. Hao, "Parameter estimation for power transformer models from time – domain data," *IEEE Transactions on Power Delivery,* vol. 1, no. 3, pp. 140 – 146, 1986, doi: 10.1109/TPWRD.1986.4307985.

[51] N. F. O. Morais, "Estimating the remaining lifetime of power transformers using paper insulation degradation," 2018.

[52] J. Rosenlind, "Lifetime modeling and management of transformers," 2013.

[53] M. Wydra and P. Kacejko, *Power system state estimation using wire temperature measurements for model accuracy enhancement*. 2016, pp. 1 – 6.

[54] M. Wydra and P. Kacejko, "Power system state estimation accuracy enhancement using temperature measurements of overhead line conductors," *Metrology and Measurement Systems,* vol. vol. 23, no. No 2, pp. 183 – 192, 2016.06.30 2016, doi: 10.1515/mms – 2016 – 0014.

[55] O. Arguence and F. Cadoux, "Sizing power transformers in power systems planning using thermal rating," *International Journal of Electrical Power & Energy Systems*, vol. 118, p. 105781, 2020/06/01/ 2020, doi: https://doi.org/10.1016/j.ijepes.2019.105781.

[56] Y. Biçen, Y. Çilliyüz, F. Aras, and G. Aydugan, "An assessment on aging model of IEEE/IEC standards for natural and mineral oil – immersed transformer," in *2011 IEEE International Conference on Dielectric Liquids*, 26 – 30 June 2011 2011, pp. 1 – 4, doi: 10.1109/ICDL.2011.6015442.

[57] "IEEE guide for transformer loss measurement," *IEEE Std C57.123 – 2019 (Revision of IEEE Std C57.123 – 2010)*, pp. 1 – 55, 2020, doi: 10.1109/IEEESTD.2020.8995817.

[58] W. U. Y, L. I. U. L, S. H. I. C, M. A. K, L. I. Y, and M. U. H, "Research on measurement technology of transformer no – load loss based on internet of things," in *2019 IEEE 8th International Conference on Advanced Power System Automation and Protection (APAP)*, 21 – 24 Oct. 2019 2019, pp. 150 – 153, doi: 10.1109/APAP47170.2019.9224961.

[59] M. T. Isha and Z. Wang, "Transformer hotspot temperature calculation using IEEE loading guide," in *2008 International Conference on Condition Monitoring and Diagnosis*, 21 – 24 April 2008 2008, pp. 1017 – 1020, doi: 10.1109/CMD.2008.4580455.

[60] "IEEE guide for loading mineral – oil – immersed transformers," *IEEE Std C57.91 – 1995,* p. i, 1996, doi: 10.1109/IEEESTD.1996.79665.

[61] "IEEE guide for loading mineral – oil – immersed transformers and step – voltage regulators," *IEEE Std C57.91 – 2011 (Revision of IEEE Std C57.91 – 1995),* pp. 1 – 123, 2012, doi: 10.1109/IEEESTD.2012.6166928.

[62] W. Ben – gang, F. Chen – zhao, L. Hong – lei, L. Ke – jun, and L. Yong – liang, "The improved thermal – circuit model for hot – spot temperature calculation of oil – immersed power transformers," in *2016 IEEE Information Technology, Networking, Electronic and Automation Control Conference*, 20 – 22 May 2016 2016, pp. 809 – 813, doi: 10.1109/ITNEC.2016.7560473.

[63] J. Li, T. Jiang, and S. Grzybowski, "Hot spot temperature models based on top – oil temperature for oil immersed transformers," in *2009 IEEE Conference on Electrical Insulation and Dielectric Phenomena*, 18 – 21 Oct. 2009 2009, pp. 55 – 58, doi: 10.1109/CEIDP.2009.5377876.

[64] V. Shiravand, J. Faiz, M. H. Samimi, and M. Djamali, "New thermal model for accurate prediction of top oil temperature of distribution transformer," in *2020 28th Iranian Conference on Electrical Engineering (ICEE)*, 4 – 6 Aug. 2020 2020, pp. 1 – 4, doi: 10.1109/ICEE50131.2020.9260946.

[65] L. Jauregui – Rivera and D. J. Tylavsky, "Acceptability of four transformer top – oil thermal models—part I: Defining metrics," *IEEE Transactions on Power Delivery,* vol. 23, no. 2, pp. 860 – 865, 2008, doi: 10.1109/TPWRD.2007.905555.

[66] L. Jauregui – Rivera and D. J. Tylavsky, "Acceptability of four transformer top – oil thermal models—Part II: Comparing metrics," *IEEE Transactions on Power Delivery,* vol. 23, no. 2, pp. 866 – 872, 2008, doi: 10.1109/TPWRD.2007.905576.

[67] O. A. Amoda, D. J. Tylavsky, G. A. McCulla, and W. A. Knuth, "Acceptability of three transformer hottest – spot Temperature models," *IEEE Transactions on Power Delivery,* vol. 27, no. 1, pp. 13 – 22, 2012, doi: 10.1109/TPWRD.2011.2170858.

[68] D. Susa and M. Lehtonen, "Dynamic thermal modeling of power transformers: further development – part II," *IEEE Transactions on Power Delivery,* vol. 21, no. 4, pp. 1971 – 1980, 2006, doi: 10.1109/TPWRD.2005.864068.

[69] D. Susa, M. Lehtonen, and H. Nordman, "Dynamic thermal modelling of power transformers," *IEEE Transactions on Power Delivery,* vol. 20, no. 1, pp. 197 – 204, 2005, doi: 10.1109/TPWRD.2004.835255.

[70] D. Simon, *Optimal state estimation: Kalman, H infinity, and nonlinear approaches*. 2006.

[71] A. Wächter and L. Biegler, "On the implementation of an interior – point filter line – search algorithm for large – scale nonlinear programming," *Mathematical programming,* vol. 106, pp. 25 – 57, 03/01 2006, doi: 10.1007/s10107 – 004 – 0559 – y.

[72] I. Lustig, R. E. Marsten, and D. F. Shanno, "On implementing mehrotra's predictor – corrector interior – point method for linear programming," *SIAM J. Optim.,* vol. 2, pp. 435 – 449, 1992.

[73] C. Rakpenthai and S. Uatrongjit, "A three – phase state estimation based on alternating optimization for power systems including conductor temperatures," *IEEE Transactions on Power Systems,* vol. PP, pp. 1 – 11, 01/01 2024, doi: 10.1109/TPWRS.2024.3353752.

[74] A. Abur and A. Gomez – Exposito, *Power system state estimation: Theory and Implementation*. 2004.

BIOGRAPHY

NAME	Dumrongsak Wongta
DATE OF BIRTH	6 March 1985
PLACE OF BIRTH	Chiang Rai Province
INSTITUTIONS ATTENDED	M.Eng. (Electrical Engineering), University of Phayao, 2017 B.Eng. (Electrical Engineering), Chiangrai College, 2009
HOME ADDRESS	97/12 Soi 6 Ban Hua Doi Santi Thasai Subdistrict Mueang Chiang Rai District Chiang Rai Province 57000
PUBLICATION	D. Wongta, J. Pahasa, C. Rakpenthai, and S. Uatrongjit, "Temperature–dependent state estimation based on constrained alternating optimization for three–phase power networks considering transformer parameters," International Journal of Electrical Power & Energy Systems, accepted. D. Wongta, S. Uatrongjit, J. Pahasa, S. Vachirasricirikul, and C. Rakpenthai, "Transformer parameters and transmission line temperatures estimation in three–phase power networks," ECTI Transactions on Electrical Engineering, Electronics, and Communications, accepted. D. Wongta, S. Uatrongjit, C. Rakpenthai, and N. Pothi. "Assessments of power systems voltage stability considering transmission line security," ECTI Transactions on electrical engineering, electronics, and communications, vol. 22, no. 2 pp. 1 – 9.

มหาวิทยาลัยพะเยา
UNIVERSITY OF PHAYAO